Thesis/
Reports
Hart,
T. C.

REDUCTION OF TOPOGRAPHIC SHADOW EFFECTS IN LANDSAT DATA BY DIVISION OF MEAN BRIGHTNESS.

by

Thomas C. Hart & Eugene L. Maxwell

1978

COOPERATIVE AGREEMENT #16-795-CA

FINAL REPORT

"Reduction of Topographic Shadow Effects in Landsat Data by Division of Mean Brightness"

Authors: Thomas C. Hart and Eugene L. Maxwell

Submitted by: Eugene L. Maxwell
Principal Investigator
Earth Resources Department
Colorado State University
Fort Collins, Colorado 80523

To: United States Forest Service
Rocky Mountain Forest and Range
Experiment Station
240 W. Prospect Avenue
Fort Collins, Colorado 80526

August, 1978

LIBRARY

MAR 21 1979

ROCKY MOUNTAIN STATION

ABSTRACT

REDUCTION OF TOPOGRAPHIC SHADOW EFFECTS IN
LANDSAT DATA BY DIVISION OF MEAN BRIGHTNESS

This remote sensing research was performed with the goal of preventing classification response degradation due to varying illumination conditions in regions of rugged topography. A ratio transformation of division by the average of all bands was used to normalize scene brightness variations.

Background material discussed includes a survey of the use of various ratio configurations, a review of computerized inventory procedural options, and a theoretical discussion of the opportunities for elimination of additive and multiplicative noise with ratio techniques.

Experimentation was limited to optical interpretation, interband correlation analysis, and training data analysis. Three versions of the ratio by division of average were processed, providing a gradient of results. Subtraction files of transformed from original data were created to help evaluate the changes in information affected by the transformations. Classification accuracies, mean vector spectral plots, means of mean vectors, standard deviations, coefficients of variation, and variable and between-class F-values were assessed in a comparative analysis of the original and transformed files.

Results indicated that the transformation effectively normalized spectral response to midrange of the dynamic range. However, the loss of brightness information consistently reduced discrimination of

vegetation cover types with a classifier using a common covariance matrix. In spite of this, there may be some utility for these procedures for inventory of simpler thematic schemes with wider spectral differences in regions of rugged topography.

Thomas C. Hart
Earth Resources Department
Colorado State University
Fort Collins, Colorado 80523
Fall, 1978

TABLE OF CONTENTS

		Page
1.0	INTRODUCTION	1
2.0	BACKGROUND ON RATIOS	4
3.0	EXPERIMENTAL SETTING	9
4.0	THEORETICAL BACKGROUND	16
5.0	OBJECTIVES, HYPOTHESES, AND APPROACH	28
	5.1 Objectives	28
	5.2 Hypotheses	29
	5.3 Approach	29
6.0	DETAILED EXPERIMENTAL DESIGN	33
	6.1 Study Area	33
	6.2 Categorical Design	35
	6.3 Transformation Processing	35
	6.4 Ground Reference Compilation	38
	6.5 Training Set Establishment	41
	6.6 Optical Studies	44
	6.7 Digital Studies	46
7.0	RESULTS	49
	7.1 Site-wide Analyses	49
	7.2 Training Data Analyses	56
	7.3 Collation of Results	74
8.0	SUMMARY AND CONCLUSIONS	75
	REFERENCES CITED	78

LIST OF TABLES

Number		Page
1	The ratio of diffuse to total global irradiance in ERTS-1 bandpasses at Sidney, 15 October, 1973.	24
2	Changing proportions of diffuse to total global irradiance, by wavelength band.	26
3	Mapping themes from categorical design phase.	36
4	Vegetation classification coincidence with illumination classes, from digitized ground reference (number of occurrences).	42
5	Vegetation classification coincidence with illumination classes, from digitized ground reference (percentage).	43
6	Interband correlation from site-wide sample.	54
7	Coding system from training categories.	57
8	Codes for the 36 training categories.	58
9	Training model mean brightness.	61
10	Band variable F-values.	63
11	Change in standard deviation in training models from original to transformed files.	68
12	Coefficients of variation for individual training models.	70

LIST OF FIGURES

Number		Page
1.	Surface orientation with respect to direct solar illumination.	20
2.	Topographic position with respect to diffuse skylight illumination.	21
3.	Spectral response curves for direct sun and indirect skylight irradiance.	23
4.	Data processing sequence.	32
5.	Aerial photo over study site.	34
6.	Vegetation ground reference map.	39
7.	Illumination ground reference map.	40
8.	A plot of training field locations superimposed upon a listed graymap of the digitized vegetation reference map.	45
9.	Grayscale displays of the original and transformed data base files.	50
10.	Grayscale displays of the difference data base files.	51
11.	First set of 12 spectral plots of training model mean vectors for original and transformed files.	65
12.	Second set of 12 spectral plots of training model mean vectors for original and transformed files.	66
13.	Third set of 12 spectral plots of training model mean vectors for original and transformed files.	67

1.0 INTRODUCTION

This research has been performed with the goal of reducing shadow effects in Landsat digital data. It addresses the need for methods to mitigate the effects of rugged topography upon sensed radiance values in the visible and near-infrared wavelengths.

In agricultural applications, the low relief topography normally presents a minimal obstacle to consistent instantaneous illumination. However, in regions of rugged terrain, the complex topography can cause an inconsistency of illumination which easily overwhelms the subtle reflectivity differences between useful cover type classes. Data processing strategies are required to minimize these masking effects of illumination changes due to topography.

Past approaches have included illumination stratification, the use of topographic data as ancillary input, and ratioing methods (Crane, 1971). The stratification technique involves a division of scene components into all appropriate combinations of cover types and topographic positions. Two prerequisites are a very detailed familiarity with local coverage patterns, and the support of a relatively comprehensive ground reference data bank. Even after the successful designation of appropriate strata, the effects of illumination differences often perturb classification of the intended themes.

To use topographic data as ancillary input, the analyst must first digitize the terrain data into a grid sample which corresponds to his digital spectral data. Subsequently, there are two choices of strategy. The first is similar to stratification, except that there is a

sequential treatment of the two scene variants: first a topographic position is computed for a given cell, and then a choice of cover type designation is made from a list of those which might be found at such a topographic position. The second treatment of terrain data involves an illumination model which calculates variations in incoming illumination as a function of topographic position. In both methods, the digitization of topographic data and its registration with spectral data incur high costs in terms of additional sources of error, analytic man-hours, and in some regions, the cost of obtaining the original terrain data.

Interband ratio techniques, on the other hand, provide mechanisms for reducing the effects of illumination variation in scanner data with no need for ancillary data. Rowan et al. (1976) found that the output image from ratio preprocessing "shows subtle reflectivity differences and concurrently minimizes radiance variations due to topography." Vincent (1972) concluded similarly that ratios can monitor subtle spectral changes, in spite of shadowing and target geometry variations. For atmospheric and system noise reduction, Crane (1971) found ratios useful because of the normalizing effects of combining more than one spectral channel. With similar logic, Wagner, et al. (1973) stated:

> "The ratioed image... is more nearly a function of terrain reflectance (or emittance characteristics) than the radiance levels recorded in any one band alone."

In the context of digitized multispectral aerial photography, Brooner and Simonett (1971) reported many advantages of ratios:

> "Normalization was carried out to reduce, if not eliminate, the effects of vignetting, partially uncompensated off-axis illumination fall off, variations in terrain reflectance with viewing angle (especially marked differences in fore- and back-lighting), and slight differences in color processing. It was based on the expectation that the ratio of reflectance in each (film) layer remains relatively stable despite these sources of film variation."

Ali and Aggarwal (1976) and Williams and Aggarwal (1976) both used a normalization of film layer densities to suppress shadowing effects and enhance subtle color phenomena for the purpose of distinguishing citrus trees from the background orchard floor.

Finally, in a strict photographic processing mode, Yost, et al. (1973) developed a method for displaying color differences independent of brightness variations using a composite of several bands in opposing positive/negative sandwiches.

2.0 BACKGROUND ON RATIOS

There are four common configurations of ratio transformations in digital image processing: 1) the simple ratio of one given band to any other given band, 2) the simple ratio of two adjacent bands, 3) the ratio of the difference between two bands divided by their sum, and 4) the ratio of a given band divided by the average of all bands. The first three types involve pairs of bands, while the fourth uses an overall average as the normalizing factor. An evaluation of the various utilities of these four options follows.

The simple ratio of two non-adjacent bands is usually used for the enhancement of scene components peculiar to a given application. The enhancement potential is associated with the possibility that the slope of the spectral curve between two bands would be more responsive than the raw band values to particular scene conditions. Many investigators of geological applications have found this to be the case for detecting reflectance differences related to chemical and mineralogical differences (Rowan et al., 1976; Podwysocki et al., 1977; Vincent, 1972, 1973; Billingsley, 1973; and Siegal and Abrams, 1976). There is a corollary advantage of the "removal of first order brightness effects due to terrain slope which perturb classifications based on absolute brightness" (Billingsley, 1973). Siegal and Abrams (1976) commented on this manifestation in more detail:

> "Although different materials may have similar MSS values due to unevenness of illumination intensity caused by topography, the ratios of their MSS bands would be different, and hence the materials should be separable."

For vegetation applications, Tucker (1977) and Rouse et al. (1974) among others, have investigated the correlation of infrared/red ratios with vegetation biomass and physiological status. Tucker (1977) has found evidence that suggests that a simple infrared/red ratio tends to normalize the soil background scene component.

However, the utility of such ratios for reduction of illumination variation effects due to topography depends on the type of shadow effects extant in the scene. In a relatively barren area where the incoming illumination is blocked by opaque geological materials, the simple ratios are effective in normalizing the topograhic shadowing. However, in more heavily vegetated areas, a larger component of the shadow, or illumination reduction, is affected by partial transmittance through plant materials. Colwell (1974) has shown that this transmittance is species and wavelength dependent. Therefore, the simple ratio response becomes less predictable with increases in the quantity and variety of vegetative cover.

Extraneous variation of this type is considered noise, in that it only masks or confuses the desired signal. Other illumination noise sources which are wavelength dependent include the changing contributions of sunlight and diffuse skylight to total illumination in each of the bands. Variations with wavelength dependency pose a serious obstacle to the use of simple ratios, since noise factors would not cancel if they changed appreciably from band to band.

However, for wavelength dependent noise, one can argue that there will be less variation in noise level between adjacent bands than between widely separated bands (Crane, 1971; and Kreigler et al., 1970). This logic is a strong rationale for limiting the paired ratio

configurations to adjacent band combinations. The adoption of such a strategy, however, does preclude the use of those separated band combinations most responsive to the given application.

Another method of normalization using only two bands is ratioing the difference over the sum. This can be used for adjacent bands (Smedes, 1971; Kreigler et al., 1970; Nalepka, 1970; and Crane, 1971) or for separated bands (Tucker, 1977; and Rouse et al., 1974). Although the experimental conditions differed,[1] there are interesting comparisons to be made between the results of Smedes (1971) versus those of Tucker (1977) and Rouse, et al. (1974). Smedes found that adjacent band simple ratios performed better than adjacent band difference/sum ratios in classifying heterogeneous vegetation cover in rough terrain. Tucker, on the other hand, used separated band combinations, and concluded that his difference/sum ratios were more responsive than the simple ratios in correlation analysis with range biomass and physiological status parameters. Rouse, et al. (1974) reported that the same difference/sum configuration responded better than the simple ratio in normalizing locational and cyclical deviations of vegetation status. It could well be the case that since Smedes used adjacent band simple ratios, his difference/sum method with those same bands resulted in excessive normalization and information loss;

---

[1] It should be noted that most of the references cited in this section have widely differing experimental constructs and objectives. The description of these studies is necessarily incomplete, and includes only those findings which pertain to the discussion at hand. For a thorough understanding of the overall context of these results, the reader is referred to the source materials themselves.

Tucker and Rouse, on the other hand, needed the difference/sum method to strengthen the incomplete normalization affected by their separated band simple ratios.

The fourth ratio type, that of the division of a single band value by the average of all bands, is the configuration that is to be evaluated in this research. In using the combination of all wavelength bands as its normalizing factor, and applying that same factor to all individual bands, the method avoids some of the vulnerability to wavelength dependent noise discussed in terms of the paired band ratios above. An additional advantage of this approach is the maintenance of original variable character. While single band values are changed to spectral curve slope data by the two band ratios, the averaging ratio normalizes each original value by a common factor, and thus the relationship of qualitative information content between bands should not change appreciably. One application of this advantage would be to use two band ratio strategies, say for the purpose of Tucker's biomass estimations, subsequent to averaging ratio normalization.

Historically, this fourth transformation type has been a standard processing option on the JPL-VICAR interactive image processing system (Billingsley and Goetz, 1973). Gillespie (1977) has characterized its use as effective for optical enhancement of lithological patterns. Automated image classification using this ratio method has not been tested at JPL.

Smedes (1971) did use this method for automated classification of aircraft scanner data and found it more effective than either simple adjacent channel ratios, or the difference/sum adjacent channel ratios.

Kreigler, et al. (1970), on the other hand, found no significant differences in the normalizing effects of the above three methods.

Hansen (1973) corroborates the findings of Kriegler, et al. (1970) in his study of digitized color film layer densities. He does maintain that ratioing techniques in general are useful for normalizing scene brightness. Brooner and Simonett (1971), Ali and Aggarwhal (1976), and Williams and Aggarwhal (1976) all used the averaging transformation exclusively, and found it to be a satisfactory preprocessor for subsequent classification of digitized color film densities.

In summary, a transformation which normalizes digital multispectral data by division of the average values has been used successfully and extensively for digital image classification of aircraft data. However, as reported in the literature, the transformation's use with Landsat data has been limited to image enhancement for optical interpretation. This research, then, is a response to the need for determining the effects of such a transformation on Landsat digital image classification, particularly in areas of rugged topography.

3.0 EXPERIMENTAL SETTING

The following discussion is a review of Landsat digital image classification techniques for inventory of natural resources. It provides a procedural framework for the application of the transformation process which is evaluated in this research.

The spectral and spatial resolutions of the satellite sensing system are first described. Landsat's multispectral scanners (MSS) detect radiance levels in four spectral bands from an altitude of 925 kilometers. The bands cover the following wavelengths:

Band 1 500-600 nanometers (green)
Band 2 600-700 nanometers (red)
Band 3 700-800 nanometers (near infrared)
Band 4 800-1100 nanometers (near infrared)

The scan line separation and the instanteneous field of view (IFOV) are approximately 79 meters wide. The continuous output of the sensors is sampled every 56 meters. This results in an effective image sample size (picture element) of approximately 1.1 acres. Digital tapes are encoded with radiance values ranging from 1 to 128 (7 bit) for bands 1, 2, and 3, and values ranging from 1 to 64 (6 bit) for band 4.

Satellite scanner data contain information in the spectral domain only. Computerized extraction of resource information from these data is only possible by keying the data to known ground conditions. Therefore, ground reference data sampling is required to establish associations between the digital multivariate radiance

patterns and useful cover type classes. Reference data may consist of either field maps or aerial photos of various scales. In either case, an effort must be made to match the spatial cover data with the corresponding digital spectral data. Since topography, and the illumination noise associated therewith, can complicate this matching effort enormously, there will be different ground reference requirements depending upon the plans for topographic variation normalization.

In concert with satellite and ground reference data concerns, the user/analyst needs to select a set of processing alternatives that suit his particular objectives. The areas of choice can be itemized as categorical design, preprocessing, class model development, and classification algorithm options.

Categorical design entails the selection of thematic objectives to serve as priorities during the class model development stage. To discuss all the guidelines for this design stage would be to digress far beyond the purposes of this research. Therefore, the reader is referred to Maxwell, et al. (1978) for a detailed discussion of this issue.

Preprocessing techniques to improve the correlation between cover and spectral classes might include: 1) the rescaling and stretching of the data to heighten contrast in optical output displays, and to render equivalent the relative levels of each band; and 2) the application of ratioing and/or spatial filtering techniques to enhance particular phenomena or to reduce extraneous variation.

Once the data are preprocessed in the chosen manner, a decision must be made among the procedural options for the development of class models. These models will be input to the classification algorithm to

serve as examples of selected classes during the mapping of the scene at large. The models themselves consist of "signatures" for each category, comprised of statistical moments (mean vectors and covariance matrices) derived from a sample of digital cells which represent the given category.

The procedures for the selection of these samples can be characterized as either supervised or unsupervised. A supervised approach involves the analyst in the designation of sample areas, or fields, for each of the classes chosen in the categorical design phase. The unsupervised procedure uses a computational algorithm to group the spectral data into clusters of statistical similarity; analyst input is limited to the assignment of restrictions in the number, size, and statistical similarity of the clusters.

Neither method alone has proven adequate over a broad range of inventory problems. The supervised procedure is weakened by the analyst's poor perspective on the interactions of complex scene components; it is too often the case that the field selection is a reflection of user categorical bias at the expense of a reduction in the ability of these models to effectively represent the inherent spectral variation of the scene. While the models themselves are of known character, their suitability as class patterns over the scene at large is always subject to question.

Conversely, the unsupervised model can be guaranteed to represent the multivariate distribution of the scene in a comprehensive manner. However, the units of such a representation may or may not have the desired congruity with thematic objectives. Furthermore, it is more

difficult to standardize the unsupervised method than the supervised method in iterative inventory efforts and change detection analysis.

There has developed from a history of these problems a consensus of opinion that: 1) a combination of approaches would produce better results; and 2) that preprocessing in terms of data normalizations and/or spatial filtering can mitigate the shortcomings on both fronts.

In the past five years, many strategies have been developed to combine the two model development options. The breadth and particulars of these strategies is beyond the scope of this study. However, the utility of data normalization in this context is pertinent.

For supervised model development, ratio normalization has been shown to reduce the need for detailed stratification within a class. Nalepka (1970) found that "preprocessing helps to extrapolate the decision rule to illumination levels not found in the training set." Smedes, et al. (1971) concluded that "preprocessing allowed the use of a single training area for each class of objects anywhere in the field of view." With less illumination variation to compensate for, the analyst can more closely approximate a comprehensive model structure.

In terms of unsupervised models, this same reduction in variation results in a simplified multivariate pattern whose clustered elements may have a higher probability of matching informational themes.

The classification algorithm, or classifier, is a computational procedure which results in the assignment of a class label to each digital cell. The bases for this assignment are similarity criteria between that cell's multivariate position and the patterns or models developed for each class in the preceding step. This procedure is commonly called pattern recognition.

These algorithms can be divided into those which are based upon distance and those which are based upon probability density. Distance is defined within the n-dimensional feature space, which is scaled in terms of the value ranges of the n variables involved in the multivariate analysis. Some distance classifiers use distance units which are directly proportional to the variable units, while others compute distance as a function of a given class model's variance in the direction of the point in feature space represented by the cell in question. In either case, that class associated with the smallest distance to the point is ascribed to the cell.

Probability density classifiers use the class model's statistical moments to compute a surface of probabilities within the feature space. These surfaces are called probability density functions. Most of the decision algorithms of this type have been derived from Bayes rule:

$$P(w_j/x) = \frac{p(x/w_j)\ P(w_j)}{\sum_{i=1}^{n} p(x/w_i)\ P(w_i)}$$

where:

n is the number of classes

w_j is the class j

x is the multivariate vector of the cell in question

$p(x/w_j)$ is the probability density function for x, given that the class is w_j

$P(w_j)$ is the a priori probability for class w_j

$P(w_j/x)$ is the a posteriori probability of class w_j, given vector x.

These a posteriori probabilities are computed for each class for each digital cell, and the cell is labeled with that class associated with the highest a posteriori probability. This is the reason for these algorithms being called maximum likelihood classifiers.

The scene classification phase is often the most expensive part of analysis of digital data in terms of computer costs. In most cases, expense rises in direct proportion to the number of classes, but in ascending geometric proportion to the number of variables. Therefore, any opportunity to reduce the number of variables will result in a significant cost savings.

Use of the averaging transformation affords such an opportunity. By incorporating within each band's transformation result the average of all bands, it is possible to calculate the value of the nth result from the other n-1 results. Therefore, the last band transformation is redundant, and may be left out of the data set during multivariate analysis. This is the approach taken by Smedes (1971), Nalepka (1970), Kreigler, et al. (1970), and Hansen (1973).

However, even though the last band transformation is redundant in a statistical context, it still describes the unique relationship between the original last band and the average of all bands. Therefore, for the purpose of optical data analysis, and, to some degree, for the purpose of rigorous digital results interpretation, there are justifications for maintaining this "extra" variable in the resulting multivariate data set. Brooner and Simonett (1971) and Billingsley and Goetz (1973) used this transformed variable configuration in their experiments.

Finally, it is possible to retain the average itself as either a replacement for the "extra" variable, or as an additional "extra" variable. Since the average represents a brightness or intensity measure for the cell, this configuration raises interesting possibilities for the separation of brightness and color, and motivates questions as to how results from such a configuration would compare with those from the original data. With no comparison with original data, Williams and Aggarwhal (1976) used n-1 normalized spectral variables plus the intensity element with highly successful consequences.

The preceding discussion has set a framework of methodological options for the application of ratio transformations.

4.0 THEORETICAL BACKGROUND

This section will contain technical material describing the factors affecting sensed radiance levels, opportunities for controlling those factors using ratio transformations, the character and effect of residual noise after transformation, and a summary section describing the overall change in data characteristics affected by the transformation.

A radiance measurement, as obtained by the satellite sensors, can be described by the following relationship:

$$N = H \cdot \frac{\rho}{\pi} \tau + N_p$$

where:

- N is the radiance level (or brightness) recorded at the sensor,
- H is the irradiance (or illumination) incident upon and integrated over the area represented by the digital cell; this is global or hemispherical irradiance, which can be further partitioned into direct sun irradiance and diffuse skylight irradiance,
- ρ is the combined reflectance (or integrated reflectivities) of all materials lying within the area represented by the digital cell; this is a dimensionless value representing the percentage of irradiance reflected; there is an assumption that the surface constitutes a diffuse or Lambertian reflector which scatters the incident radiation uniformly into a hemisphere,
- τ is the atmospheric transmittance coefficient, expressed as that percentage of $H \cdot \rho$ energy which is passed through the atmosphere,
- N_p is the path radiance, or that portion of N which is contributed directly by the atmosphere.

The relationship of these factors is described in the above equation for one band only. As will be discussed below, all the factors are a function of wavelength. Therefore, a subscript λ_i should be distributed throughout the equation.

In the case of the Landsat system, there are four N measurements recorded for a cell. While each N can be conceptualized as a brightness reading, collectively the four N's represent a coarse color response defined by the shape of the response variation across the bands. The term "color" is used by analogy to our own eyes' integration of multi-wavelength radiance patterns into a singular color sensation. In the multivariate digital mode, the response curve is analagous to our eyes' color sensitivity. The shape of the digital response curve can be considered independent of any intensity determination defined by an offset level on the collective brightness scale.

Overall, among the factors affecting radiance levels at the sensors, only one, reflectance, is related to ground cover phenomena. Therefore, efforts to normalize radiance values are pointed toward the isolation of scene reflectance variations, from which discrimination of cover types would then be enhanced.

The general strategy is to ratio two radiance levels such that multiplicative factors are cancelled if they are consistent for both radiance values. Before this is possible, however, the additive factor N_p, must be eliminated so that numerator and denominator are reduced to singular terms between which cancellation can occur. This additive path radiance factor is definitely of significant magnitude. Ross (1973) suggests that as a minimum, 10% of recorded radiance in

the visible wavelengths consists of "haze, or air light" from aircraft altitudes of around 5000 feet. Certainly the additive contribution would be greater from satellite platforms.

The additive term is reduced to an insignificant level by the dark object subtraction process (Kriegler et al., 1970; Vincent, 1972, 1973; and Chavez and Mitchell, 1976). By assuming that the darkest object in the scene in a given band is a perfect absorber of all incident irradiance in that band, one can designate the radiance level recorded at the sensor as the additive level of path radiance. Subsequently, the subtraction of this level in this band from all cells in the scene will yield an additive term correction. The weakness of the perfectly absorbing object assumption causes an over-correction, i.e., too high a level of subtraction; the implications of this will be addressed later.

The radiance equation, now in its reduced state, is written as $N = \frac{H\rho\tau}{\pi}$, because irradiance impinges upon the surface before the reflected response is attenuated by the atmosphere. It is important to note that the H and τ factors have separate effects upon the radiance levels.

The isolation of reflectance differences between digital cells, then, is dependent upon control of those other radiance factors which also change from cell to cell. The atmospheric transmittance coefficient can be assumed constant over an area of the size of that studied in this research, so that there is no concern for the normalization of this factor. Irradiance, on the other hand, does vary geographically. While the potential for illumination from either the

sun or diffuse skylight is constant over a small region, variations in surface characteristics can change the effective illumination from cell to cell in several ways.

First, the surface orientation with respect to sun angle is diverse in regions of complex topography. Figure 1 shows a typical case where the effective direct sun irradiance on the surface falls off as orientation shifts away from a position normal to the sun angle. The density of tick marks for each orientation is diagrammatic of the changing effective sun irradiance. On the left side of the figure, topography has blocked all direct irradiance from the sun for surfaces B, C, and parts of A. The direct sun irradiance that does impinge upon the surface is spread out far more than D than at F. This variation in direct illumination can be considered independent of wavelength.

A similar, spectrally independent effect occurs when topography reduces the effective diffuse sky irradiance. Figure 2 is a two-dimensional illustration of the variation in available hemispherical sky irradiance as a function of topographic position. The length of arc associated with each topographic position is a planar representation of the available proportion of maximum sky irradiance at that position. Note that while positions A, and B occupy the same slope, their heights on that slope relative to the surrounding topography are a factor in the amount of available diffuse sky irradiance. This effect, in general, can be thought of as a diffuse illumination shadowing factor.

The two sources of illumination add together to form the total illumination for any one image cell. Because the reduction in

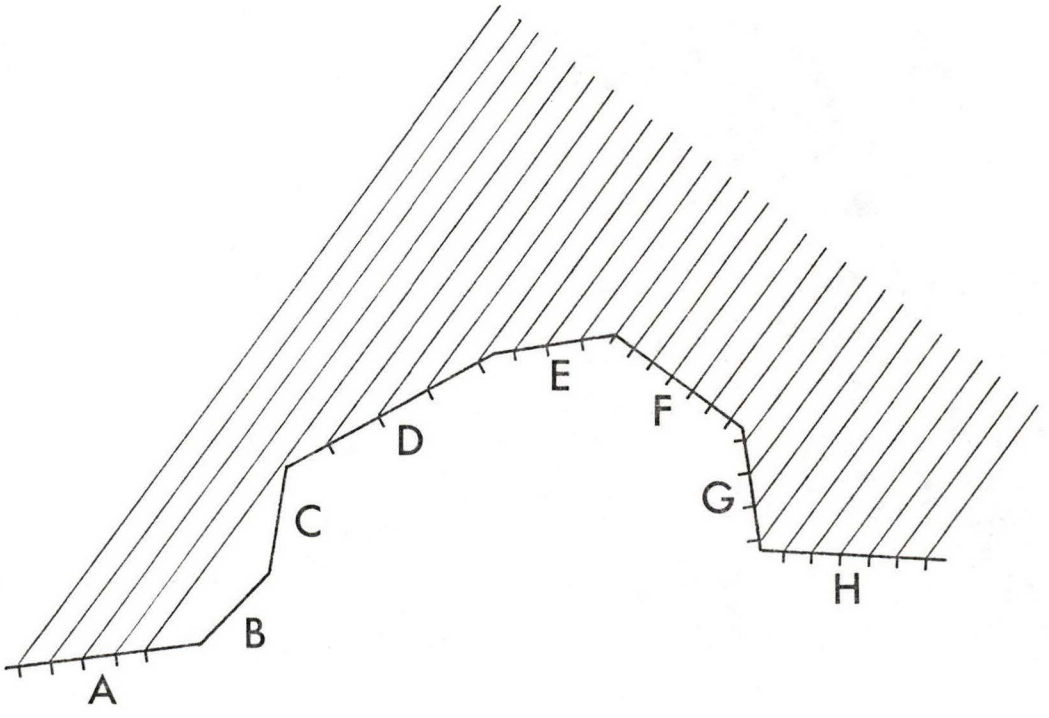

Figure 1. Surface orientation with respect to direct solar illumination.

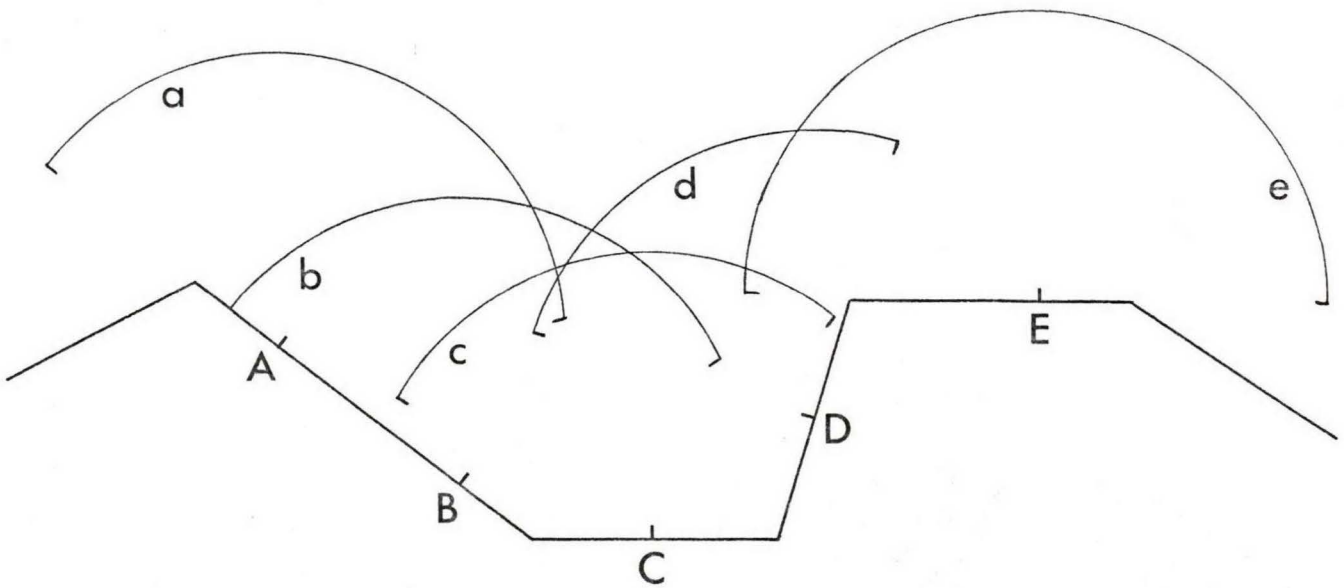

Figure 2. Topographic position with respect to diffuse skylight illumination.

illumination from either source derives from different characteristics of the cell's topographic position, the topographic influence on each source is not a common element which can be factored exterior to the summation. However, to the degree that the proportion of illumination reduction is the same for all bands within a given cell, the topographic influence on illumination will cancel in a ratio configuration.

The imperfections of this cancellation are due to wavelength dependence of the variations in total illumination. First, that portion of irradiance which is transmitted through vegetation is highly variable over vegetation type and wavelength (Colwell, 1974).

Second and more important is the effect of summing different proportions of sunlight and skylight. While the spectral response curves for the two sources are individually constant over a region, the two curves are shaped differently, especially in the infrared (Figure 3). Therefore, since these different responses are summed variously as the proportions of each source change from cell to cell, there is geographical variation in the spectral character of total illumination.

Since this spectral variation inhibits the cancellation of topographic effects in a ratio technique, it is considered noise, whose relationship to variations in cell reflectance is of prime importance.

Duggin (1974) found that "sky irradiance is generally far less than 15% of the global irradiance." His data (Table 1) give examples of the spectral dependency of the skylight/sunlight relationship.

Using Duggins's data it is possible to calculate an example of the noise variations. Assuming that the entry items are in chronological order through the day, the first entry would correspond most closely to the time of a Landsat overpass. In terms of brightness

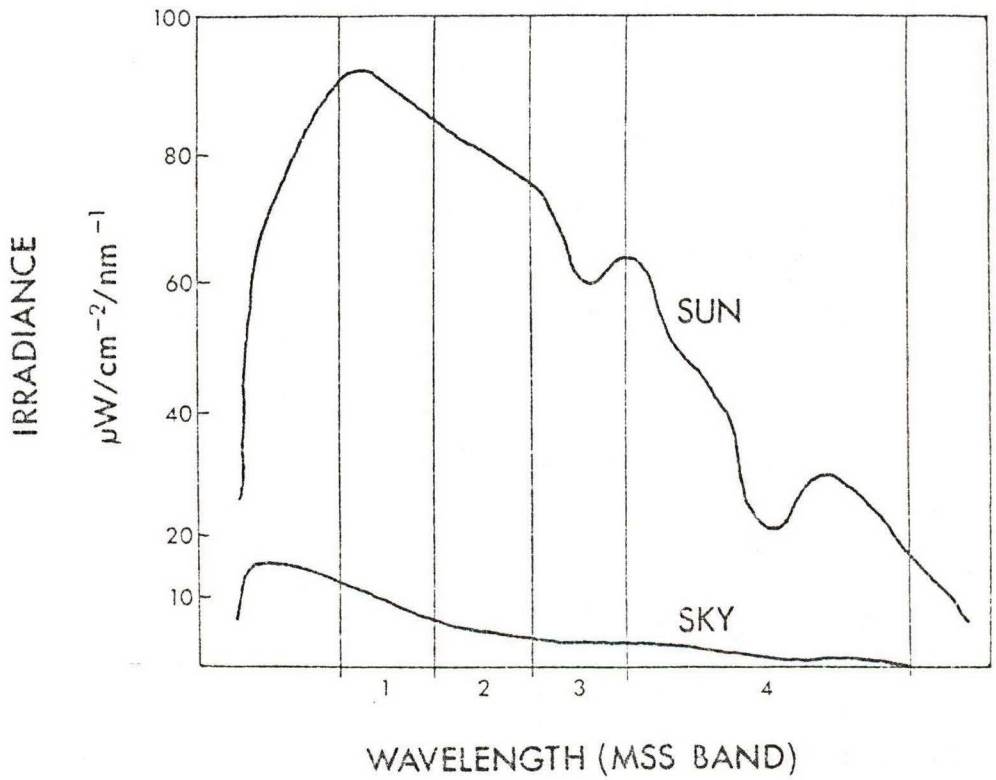

Figure 3. Spectral response curves for direct sun and indirect skylight irradiances (after Yost and Wenderoth, 1969).

Table 1. The ratio of diffuse to total global irradiance in ERTS-1 bandpasses at Sydney, 15 October, 1973 (Duggin, 1974).

Sun Angle	MSS-1 500-600mm	MSS-2 600-700mm	MSS-3 700-800mm	MSS-4 800-1050mm
45	.082	.055	.038	.021
40	.079	.055	.036	.022
35	.067	.044	.030	.017
30	.070	.048	.034	.021
25	.082	.058	.042	.031
30	.127	.105	.090	.079
35	.155	.118	.098	.084
40	.200	.166	.151	.130
45	.124	.088	.062	.044
50	.140	.103	.079	.059
55	.149	.105	.074	.049
Mean	.116	.086	.067	.051

level, the drop in irradiance from sunlit to shadowed would be 81.8%, 94.5%, 96.2% and 97.9% for the four bands. The mean reduction in irradiance, then, is 92.6%, and the maximum variation from this mean is (92.6-81.8)/(92.6)=11.7%.

In a spectral context, however, the noise presents a far more serious problem: the differential amplification of the spectral curve. From a normalization of the ratios given in Table I, Table II shows that variations in band 4, for the same entry, are nearly four times more muted than variations in band 1, as illumination conditions change from totally sunlit to totally shadowed. Using the same noise calculation off of the mean, the maximum amplification variation is (3.90-2.33)/(2.33)=67.3%.

Both of the above results show a stronger residual brightness level for the shadowed case in the shorter wavelength bands. However, by removing the additive path radiance term, an assumption of a perfect absorber is made for the dark object. This assumption is more imperfect for the shorter wavelength bands, resulting in higher over-correction, or over-subtraction, in those bands. Therefore, the additive correction does lessen the inconsistency of the residual brightness level. The degree of this fortuitous compensation is incalculable from the available data.

In summary, the opportunities for reduction of brightness variations due to topography are promising with ratio techniques. However, since there are wavelength dependencies associated with this normalization, the changes in reflectance from cell to cell will be compounded by a bias of differential spectral curve amplification. Therefore, the need for stratification by illumination condition is

Table 2. Changing proportions of diffuse to total global irradiance, by wavelength band (MSS 4 is baseline)(after Duggin, 1974).

Sun Angle	MSS-1	MSS-2	MSS-3	MSS-4
45	3.90	2.62	1.81	1.00
40	3.59	2.5	1.64	1.00
35	3.94	2.59	1.76	1.00
30	3.33	2.29	1.62	1.00
25	2.65	1.87	1.35	1.00
30	1.61	1.33	1.14	1.00
35	1.84	1.40	1.17	1.00
40	1.54	1.28	1.16	1.00
45	2.82	2.00	1.41	1.00
50	2.37	1.75	1.34	1.00
55	3.04	2.14	1.51	1.00
Mean	2.27	1.69	1.31	1.00

not completely eliminated, and a caution against defining themes of similar reflectance for inventories over rugged terrain is advised.

With these constraints accounted for, it should be possible to accentuate the different spectral responses between materials using ratios. This is especially true for the ratio using an average of all bands, since through its common factor it avoids the compound vulnerability to spectral dependent noise exhibited by simpler ratios.

5.0 OBJECTIVES, HYPOTHESES, AND APPROACH

This section sets forth the objectives and hypotheses which were motivated by issues discussed in the first four sections, and describes both the planned and achieved experimentation which grew out of the objectives and hypotheses.

The evaluation of the transformation should be implemented in light of the following two theoretical conclusions.

1. The transformation's cancellation of brightness magnitude is non-specific of brightness source, and does not ensure the preservation of the brightness component of reflectance characteristics.
2. Spectral dependencies associated with the varying illumination conditions cause some spectral curve deviation from an ideal response taken under consistent illumination conditions.

5.1 Objectives

The overall objective of this study was to assess the effects (beneficial and negative) of a ratio transformation (involving the average radiance of all bands) for supervised classification of natural cover types in high relief terrain. The goal was a reduction in misclassification due to shadowing effects.

More specific objectives included:

A. an evaluation of the degree of illumination consistency affected by the transformation,

B. an assessment of the impact on classification accuracy from the transformation's suppression of brightness variations

within the scene, and from the transformation's effects upon multispectral response.

5.2 Hypotheses

1. Vegetation cover types are separable solely on the basis of color or spectral character, as distinguished from brightness characteristics.
2. A transformation which normalizes with an average of all bands eliminates brightness variation and enhances spectral response.
3. Due to the cancellation of brightness magnitude information, the transformed file will show higher classification success with those classes whose separability relies upon a unique multivariate character, and will show lower classification success for those classes which are distinguished primarily by brightness levels.

5.3 Approach

The experimental design was of much wider scope before time restrictions combined with software problems to cut short the testing of the transformation's effects. Since a substantial effort went into planning and expanded testing, it will be described before the actual completed experimentation is addressed.

The overall design can be split into optical and digital sections, and the digital section can be split into supervised and unsupervised elements. The optical testing, as planned, included the evaluation of black and white single band graylevel prints, the color combining of 70 mm positive transparencies of these prints, and finally an

isoluminous processing test to create analog color displays with brightness variation removed (Yost et al., 1973), to compare with the digital transformation results.

The digital testing was to begin with scene-wide interband correlation analyses. Then from cellularized ground reference files for vegetation and illumination patterns over the site, a stratified training set would provide a reliable sampling of scene variation. With this sampling, supervised tests of the separability of cover types were possible for both original and transformed files. Plans were made to extend this separability testing to the difference files (resulting from the subtraction of transformed from original) to yield indications of class distinctions which were sacrificed in transformation. Finally, a supervised test of cover type separability using combined transformed/difference files would have yielded interesting results on the potential for increased classification accuracy with a separation of color and brightness information.

The unsupervised tests would have involved the same training set as a single data set for clustering. Software was designed, but unfortunately never implemented, to compress all the dispersed irregular training fields into a single rectangular array, whereupon it would be clustered as a whole, then unpacked and redisplayed in its original spatial geometry in terms of the clustering results. In this manner, the clustering would indicate: 1) to what degree our original thematic categorization "fit" the spectral variation of the scene, and 2) to what degree the transformations caused a shift in the correlation of the spectral patterns to the vegetation and illumination patterns.

With class models optimized through the indications of both supervised and unsupervised results, scene-wide classifications would be run for original and transformed files, and verified against the cellularized ground reference to yield summary results on the effects of the transformations on classification accuracy.

Figure 4 describes the processing which was actually undertaken. A detailed description of the steps is found in section 6.0.

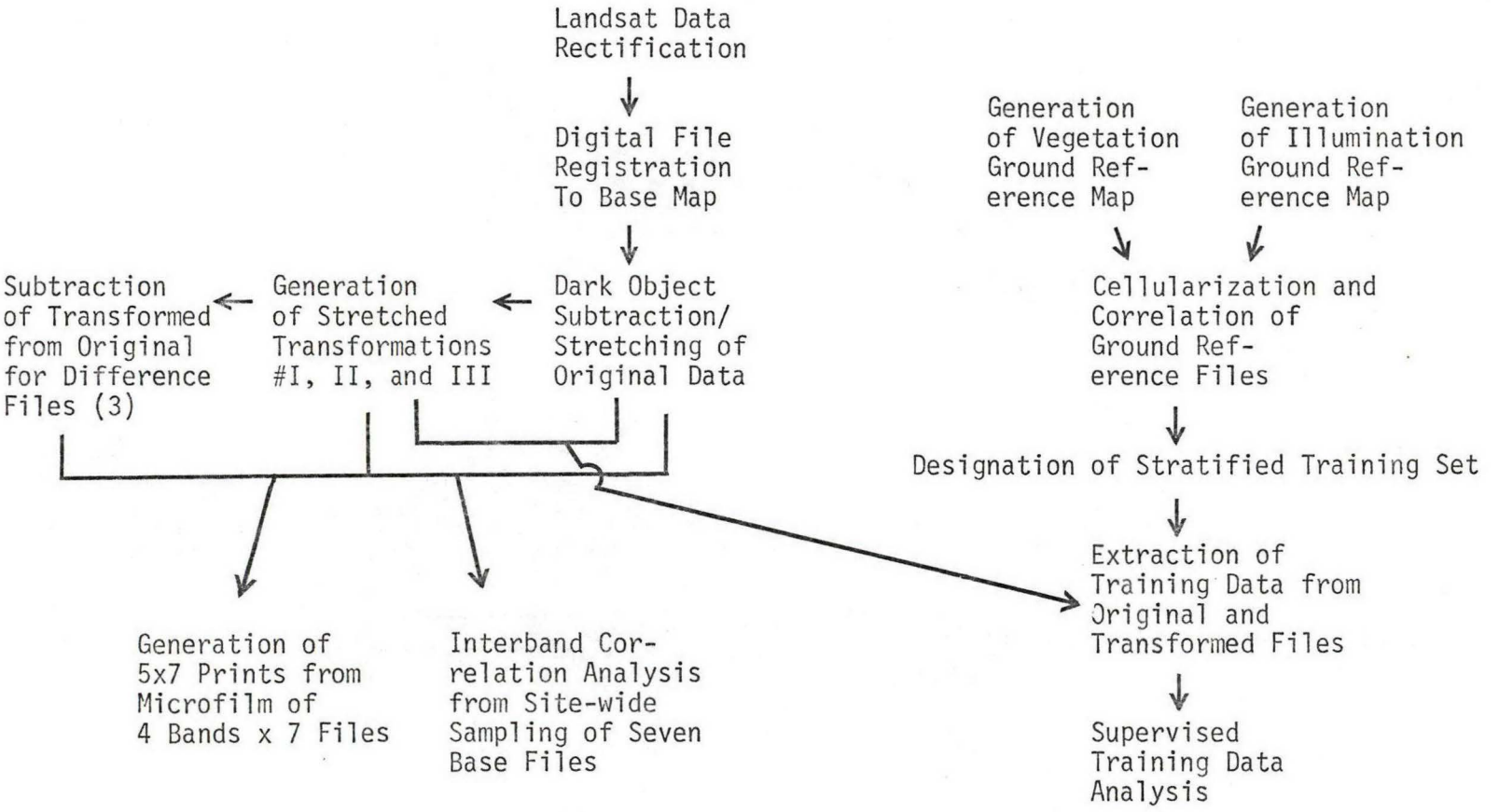
Landsat Data Rectification
Digital File Registration To Base Map
Dark Object Subtraction/ Stretching of Original Data
Generation of Stretched Transformations #I, II, and III
Subtraction of Transformed from Original for Difference Files (3)
Generation of 5x7 Prints from Microfilm of 4 Bands x 7 Files
Interband Correlation Analysis from Site-wide Sampling of Seven Base Files
Generation of Vegetation Ground Reference Map
Generation of Illumination Ground Reference Map
Cellularization and Correlation of Ground Reference Files
Designation of Stratified Training Set
Extraction of Training Data from Original and Transformed Files
Supervised Training Data Analysis

Figure 4. Data processing sequence.

6.0 DETAILED EXPERIMENTAL DESCRIPTION

6.1 Study Area

The study area straddles the edge of the Front Range foothills immediately west and north of Bellevue, Colorado. The eastern 1/3 is characterized by irrigated agricultural land use, except for shrubland on discontinuous hogback features. The western 2/3 contains highly dissected granitic terrain, with elevations ranging from 5200 to 7500 feet. Ground cover in the western sector is dominated by ponderosa pine, with a large variation in crown closure and understory characteristics. Meadows, mountain mahogany, Douglasfir and isolated cottonwood riparian complexes represent the communities of local extent in the mountainous portion of the site.

The area as a whole is roughly 4.5 miles north-south, and 5.75 miles east-west, for an approximate total of 26 square miles, or slightly less than 1/2 of a 7.5 minute quad. It is bounded on the east by the township line separating R.69 W. and R.70 W., on the north by an east-west line running just north of the Kramer Ranch buildings on U.S. 287, on the west by a north-south line passing the east edge of the meadow on top of the west branch of Boyd Gulch, and on the south by an east-west line passing over the mapped spring on the north shoulder of the Labeau Gulch canyon mouth.

Upon rectification and registration of the Landsat digital data to the map, the digital cellular grid within the site boundaries was comprised of 99 lines and 150 columns, for a total of 14,850 cells. Figure 5 gives an aerial view of the site.

Figure 5. Aerial photo over study site (approximate scale: 1/75,000).

6.2 Categorical Design

After repetitive surveys of the study area, the categorical structure was established as shown in Table 3.

The conifer forest class structure was designed to be insensitive to species composition because of the heterogeneity of species mixture, and the infeasibility of obtaining reliable ground reference on this basis. Cottonwood and aspen were grouped due to the predicted similarity of their spectral characteristics. Mountain shrub was split into a mesic subclass dominated by chokecherry, and a xeric subclass dominated by mountain mahogany and bitterbrush. Meadow/agriculture comprised a single class at the design stage due to a lack of ground reference relating the condition of the meadows and grasslands, and the cropping status of agricultural areas, at the time of Landsat overpass. Vegetation status ratio analysis with selected areas established a gradient of herbaceous productivity classes later in the project. The barren and water classes rounded out a 13-unit categorical structure.

6.3 Transformation Processing

Before the original data were transformed, linear contrast stretching was performed for three reasons. First, by rescaling the original data spread in each band to an effective range of 1 to 200, common to all bands, the potential contribution of each band to an average was equalized, so that the average would be spectrally unbiased. Secondly, by eliminating the offset from scene-wide band histograms, stretching achieved the removal of the additive path radiance influence through dark object subtraction. Thirdly, the constancy of a 1 to 200 actual data range provided a useful reference to evaluate any isolated data

Table 3. Mapping themes from categorical design phase.

1.0 Forest

- 1.1 Non-specific conifer
  - 1.1.1 Tree crown closure greater than 80%
  - 1.1.2 Open crown with lush vegetative understory
    - 1.1.2.1 Tree crown closure between 50% and 80%
    - 1.1.2.2 Tree crown closure between 15% and 50%
  - 1.1.3 Open crown with dry vegetative understory
    - 1.1.3.1 Tree crown closure between 35% and 80%
    - 1.1.3.2 Tree crown closure between 10% and 35%
  - 1.1.4 Open crown with rock understory
    - 1.1.4.1 Tree crown closure between 30% and 60%
    - 1.1.4.2 Tree crown closure between 10% and 30%
- 1.2 Cottonwood/aspen

2.0 Mountain shrub

- 2.1 Mesic
- 2.2 Xeric

3.0 Meadow/agriculture

4.0 Disturbed/excavation/bare rock

5.0 Water

element, as well as derived statistics, in terms of the data as a whole.

From this stretched original data file, three transformations involving the average of all bands were performed:

$$\text{SIMP:} \quad t_i = X_i / \left(\sum_{i=1}^{4} X_i / 4 \right)$$

$$\text{NUMS:} \quad t_i = (X_i)^2 / \left(\sum_{i=1}^{4} X_i / 4 \right)$$

$$\text{DENS:} \quad t_i = X_i / \left(\sum_{i=1}^{4} X_i / 4 \right)^2$$

The three transformations established a gradient, NUMS → SIMP → DENS, from emphasis of original data through a simple ratio of band to average to an emphasis on the average normalizing factor. The effects of the central transformation would become more apparent in the context of the effects of the extremes of this gradient.

The transformation processing for each algorithm involved a two step process. First, resultant decimal values were sampled and histogrammed for each band for the entire site. Stretch factors for the transformed results were then derived from these histograms, and inserted into the algorithms for a rerun. This produced resultant files with actual ranges of 1 to 200, matching the stretched original base file.

Finally, difference files were produced by subtracting transformed from original values and adding 100. These three difference files, then, represent the data patterns which were eliminated as a result of the transformations.

In all, seven Landsat base data files were created consisting of consisting of stretched original data, three stretched transformations, and three difference files.

6.4 Ground Reference Compilation

The ground data needs for the study were split into vegetation and illumination concerns, on the assumptions that: 1) changes in vegetation, as defined in the categorical design stage, represented the controlling factors for cellular reflectance, and 2) that changes in illumination due to topography represented the principal noise element in the translation of reflectance characteristics into sensed radiance.

The vegetation reference map (Figure 6) was generated from photo-interpretation of aerial photography. Black and white panchromatic and color infrared photos, ranging in scale from 1/20,000 to 1/60,000 gave full stereo coverage over the site; their flight dates included the months of January, April, June, and September. Mapping was performed in terms of the categories outlined in Section 6.2, with adequate locational control keyed to the road network in the eastern portion, and to the highly dissected topographic patterns in the western portion.

The illumination map (Figure 7) was derived directly from 1/24,000 scale topographic maps. While the result bears some resemblance to an ecological aspect map, its sole purpose was to describe instantaneous illumination variations across the site. The sun elevation and azimuth at the time of the Landsat overpass was 54° and 119°, respectively. A one-inch grid was drawn with the azimuth heading as its diagonal, so that, when placed beneath the topographic map on a light table,

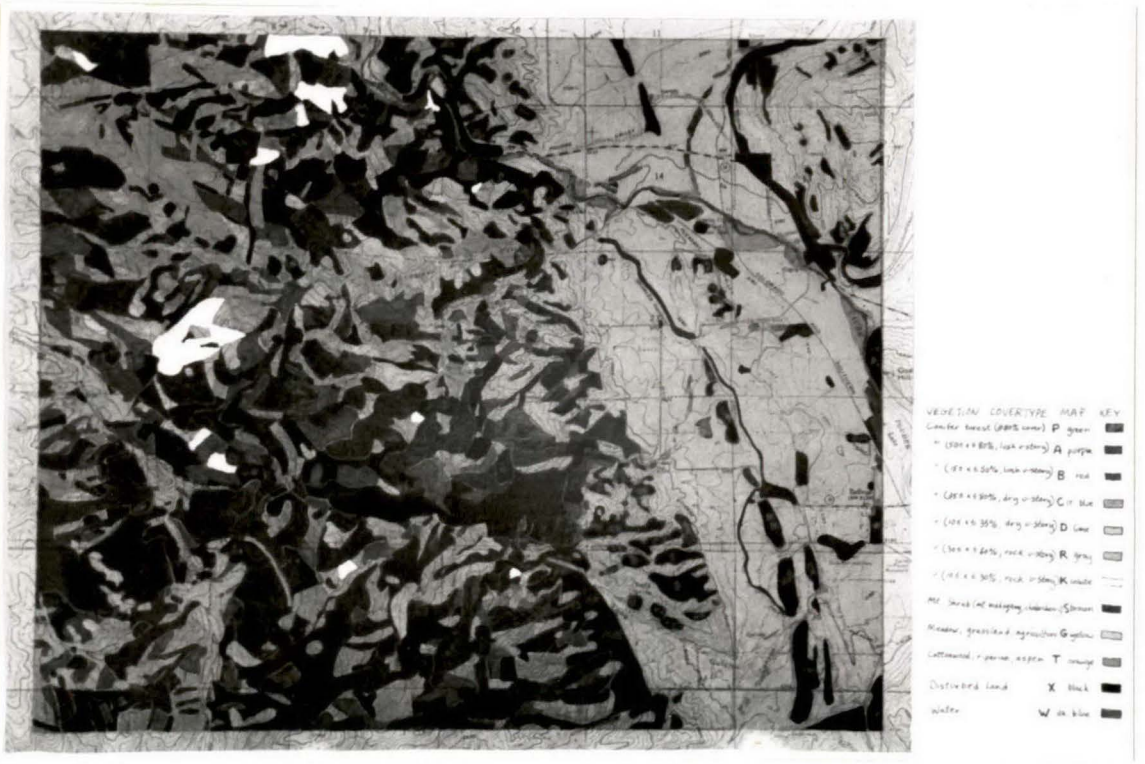
VEGETATION COVERTYPE MAP KEY
Conifer forest (>80% cover) P green
(>80% cover, high r-storey) A purple
(>80% cover, low r-storey) B red
(>80% cover, dry r-storey) C lt. blue
(10% < 35% dry r-storey) D blue
(10% < 35% rock r-storey) R gray
(<10% rock r-storey) K white
Distributed land X black
water W dk blue

Figure 6. Vegetation ground reference map.

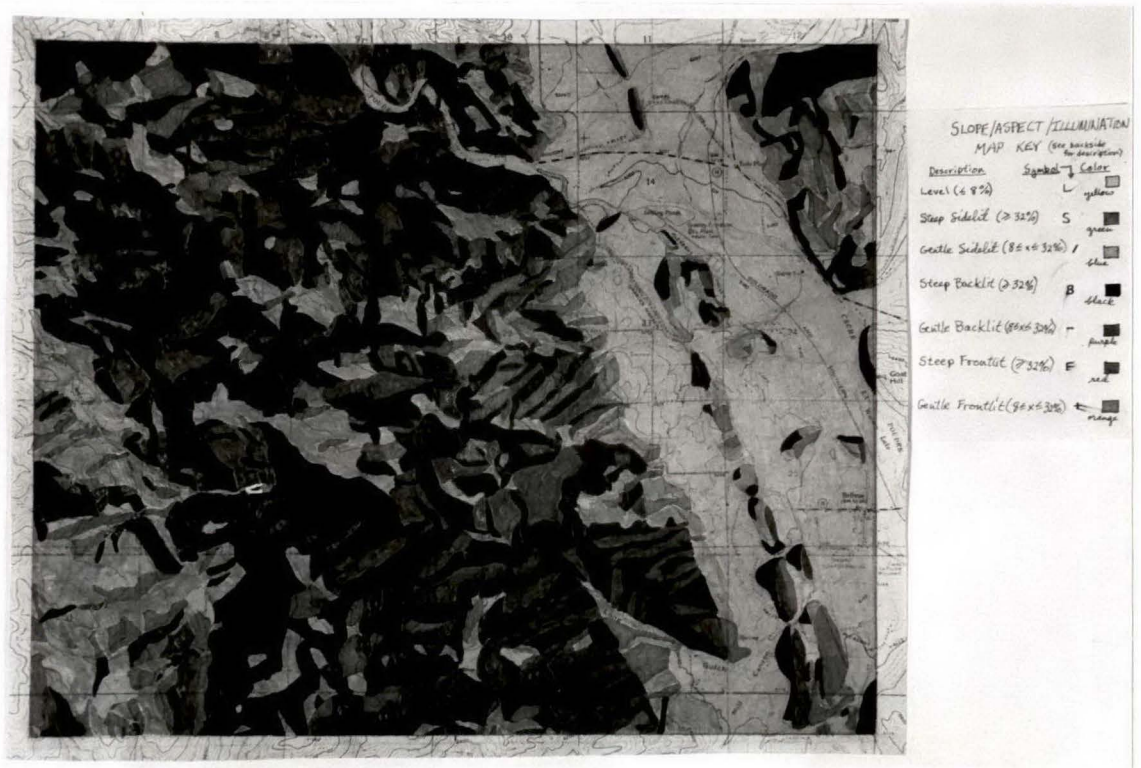

Figure 7. Illumination ground reference map.

the grid lines represented tangents of the boundary points on contour lines between front, side, and back lighted classes. Slope was also determined directly from the toposheets, with level, shallow, and steep classes corresponding to $\geq$ 1/4 inch, $<$ 1/4 inch and $>$ 1/16 inch, and $\leq$ 1/16 inch contour spacings. These three classes, then, represented $\leq$ 8%, $>$ 8% and $<$ 32%, and $\geq$ 32% slope categories, as per conversions given in Thrower and Cooke (1968). Overall, seven classes of illumination potential were mapped.

The two reference maps were then cellularized onto a Landsat grid, and were keypunched. A program was written to change the symbols assigned to each class, and by this procedure, various grayscale maps were output to a line printer by simply listing the card decks.

The principle use of these reference file card decks was to create a medium for cellular comparison of the reference files. Program MATCH was written to generate coincidence matrices for the two files. This output (Tables 4 and 5) yielded a correlation baseline between the vegetation and illumination patterns over the site, and established from this correlation the details of the need for vegetation stratification by illumination in lieu of normalizing transformations.

6.5 Training Set Establishment

For any test of the transformations' effects upon classification results, it is useful to define a sample for each class representing the breadth of variation within that class. Furthermore, the supervised classification tests in this study require that training sets be established as models for input to the classifier.

Table 4. Vegetation classification coincidence with illumination classes, from cellularized ground reference files (number of occurrences).

		SET INTERSECTION IN NUMBER OF OCCURANCES						
		L	S	/	B	-	F	+
	SUBTOTALS	3527	3996	2388	1111	594	1877	1357
P	2485	29	1160	457	390	242	109	98
A	1221	38	478	230	123	61	177	114
B	1425	51	448	344	90	74	239	179
C	1574	41	569	189	93	24	373	285
D	159	4	60	18	7	0	48	22
R	398	6	182	18	94	7	73	18
K	183	7	58	12	11	2	91	2
S	1593	58	634	206	137	35	423	100
G	5203	2771	376	888	156	143	338	531
T	132	118	5	5	1	1	0	2
X	357	291	25	19	8	5	5	4
W	120	113	1	2	1	0	1	2

TOTAL NUMBER OF CASES IS 14850

Table 5. Vegetation classification coincidence with illumination classes, from cellularized ground reference files (percentage - top number is % of column class found in row class and bottom number is vice versa).

		SET INTERSECTION IN PERCENT						
		L	S	/	B	-	F	.
	PORTIONS	24.	27.	16.	7.	4.	13.	9.
P	17.	1: 1:	29: 47:	19: 18:	35: 16:	41: 10:	6: 4:	7: 4:
A	8.	1: 3:	12: 39:	10: 19:	11: 10:	10: 5:	9: 14:	8: 9:
B	10.	1: 4:	11: 31:	14: 24:	8: 6:	12: 5:	13: 17:	13: 13:
C	11.	1: 3:	14: 36:	8: 12:	8: 6:	4: 2:	20: 24:	21: 18:
D	1.	0: 3:	2: 38:	1: 11:	1: 4:	0: 0:	3: 30:	2: 14:
R	3.	0: 2:	5: 46:	1: 5:	8: 24:	1: 2:	4: 18:	1: 5:
K	1.	0: 4:	1: 32:	1: 7:	1: 6:	0: 1:	5: 50:	0: 1:
S	11.	2: 4:	16: 46:	9: 13:	12: 9:	6: 2:	23: 27:	7: 6:
G	35.	79: 53:	9: 7:	37: 17:	14: 3:	24: 3:	18: 6:	39: 10:
T	1.	3: 89:	0: 4:	0: 4:	0: 1:	0: 1:	0: 6:	0: 2:
X	2.	8: 82:	1: 7:	1: 6:	1: 2:	1: 1:	0: 1:	0: 1:
W	1.	3: 94:	0: 1:	0: 2:	0: 1:	0: 0:	0: 1:	0: 2:

In order to assess the effects of illumination changes on vegetation signatures with respect to both original and transformed data, illumination subclasses of each vegetation type were created using the set intersection analysis results. This yielded 36 stratified categories. The actual sample site selections were achieved by overlaying the two reference files, and selecting from photos appropriate sites whose homogeneity, size, obvious location, and subtle gradient boundaries provided minimal risk of mistaken cellular identity. Software which permitted the definition of fields with irregular cellular arrangement helped to achieve these objectives. While the average field size was slightly under 7 cells, the entire sample for each strata was never less than 30 cases. A gradient of strata character was selected for the purpose of building a normally distributed class model, inasmuch as was possible. Figure 8 shows the set of fields.

The selection of grassland and agricultural training fields was inhibited by a lack of photo reference for the Landsat overpass period. Since there was no other basis to assess herbaceous stand condition, the herbaceous areas were stratified into three levels of productivity based on a MSS7/MSS5 ratio analysis of selected fields.

The 36 categories were represented by 211 training fields containing 1435 digital cells. This represents a 9.7% sample of the entire site.

6.6 Optical Studies

Graylevel displays of single bands over the seven base files were compared to assess: 1) the reduction of topographic patterns in the transformed files, 2) the consistency of displays across all bands

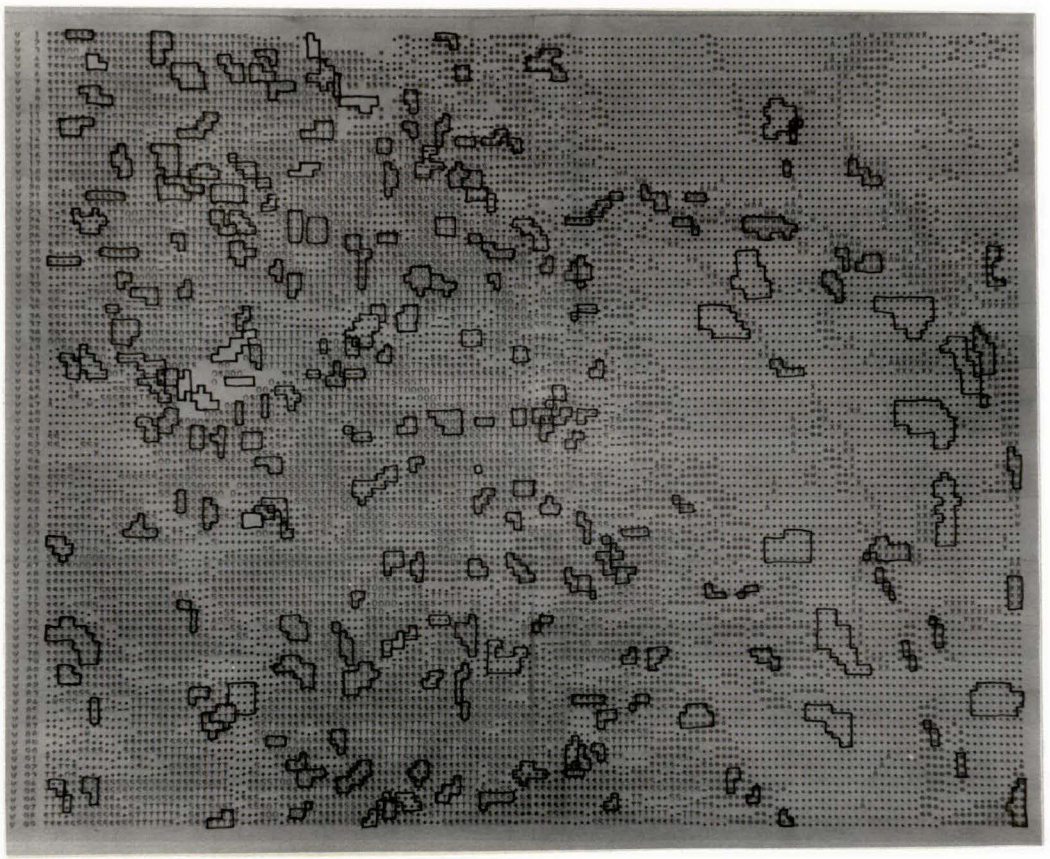

Figure 8. A plot of training field locations superimposed on a listed graymap of the cellularized vegetation ground reference map.

in the difference files, and 3) the presence of noise patterns (either as high frequency patterns, or as radiometric striping) in the transformed and difference files.

These optical interpretations were carried out in tandem with the analysis of the site-wide interband correlation results generated in the digital studies.

6.7 Digital Studies

The digital studies can be separated into evaluations of site-wide interband correlation changes between original, transformed, and difference files, and the analysis of training data with identical sets compared between original and transformed files.

The site-wide correlation data were generated using a sampling of the digital grid of every ninth line and every ninth column. These data were used to assess the removal of brightness patterns common to all bands, and the enhancement of specific multispectral patterns due to transformation.

Training data sets from each of four files were analyzed using a program called STATGEN, derived from the Biomed routine BMD07M. This program first computes means and standard deviations for each band of each input category sample. From the mean vector output, spectral plots for each class over the four files were drafted to provide a more interpretable format for evaluating the change in class mean vectors. Each mean vector was itself averaged as well, yielding a simple measure of overall brightness response. The standard deviation outputs were compared, and a difference table was generated for each

transformation's change from the original in each class. Lastly, coefficients of variation were computed for all classes on all files.

After generating mean vectors and standard deviation vectors, STATGEN proceeds through a stepwise discriminant analysis of the group of input categories. While the program computes statistics for each step, or for each feature space extension, the only statistics which will be discussed in this report are those generated from the full four-variable context; this provides the only medium for sound comparison between files whose relationship is defined, at least in part, by an average of all variables.

Therefore, the between-class F-matrices generated after inclusion of the last variable were the only outputs of the four of this type which were evaluated. Similarly, the classification summaries with all variables included were the only sources of classification accuracy figures, both in terms of each class and of the training set as a whole. Finally, while individual F-values for each variable were computed before the discriminant analysis, of the F-values generated within the stepwise context, only the final accumulated versions were used.

It should be noted that this routine uses a shared within-groups covariance matrix, common to all categories, for computing probability densities and F-values. The assumption that all classes used in this research have approximately the same-shaped distribution in feature space is subject to question. However, in light of the fact that these results were used for comparative purposes between radically different data treatments, it is justifiable, and perhaps advisable,

that shared covariance matrices were employed in these tests of general classification capabilities.

The following section will discuss the results and significance of the outputs described above.

7.0 RESULTS

The following discussion will concentrate on the differences between the original data's response and the corresponding results from the simple transformation. Comparisons with the two "extreme" versions of the transformation will be limited to response patterns which constitute a definite gradient of effects.

To appreciate the implications of the following results, a thorough familiarity with the three transformation algorithms is required:

1. SIMP - a simple ratio of one band to the average of all bands
2. NUMS - (SIMP with numerator squared) the square of the band divided by the average
3. DENS - (SIMP with denominator squared) the band divided by the square of the average

The difference files, created by subtracting the results of the above three transformations from the original file, are designated as ΔS, ΔN, and ΔD, respectively.

7.1 Site-Wide Analyses

Under this heading are the results derived from the optical display interpretations and the interband correlation statistics.

The grayscale output for the original and transformed files is shown in Figure 9, while the grayscale displays for the difference files are shown in Figure 10.

Overall, the optical displays show a pattern of increasing brightness suppression as the gradient progresses from original to NUMS to SIMP. This is shown most obviously by the consistency of scene-wide

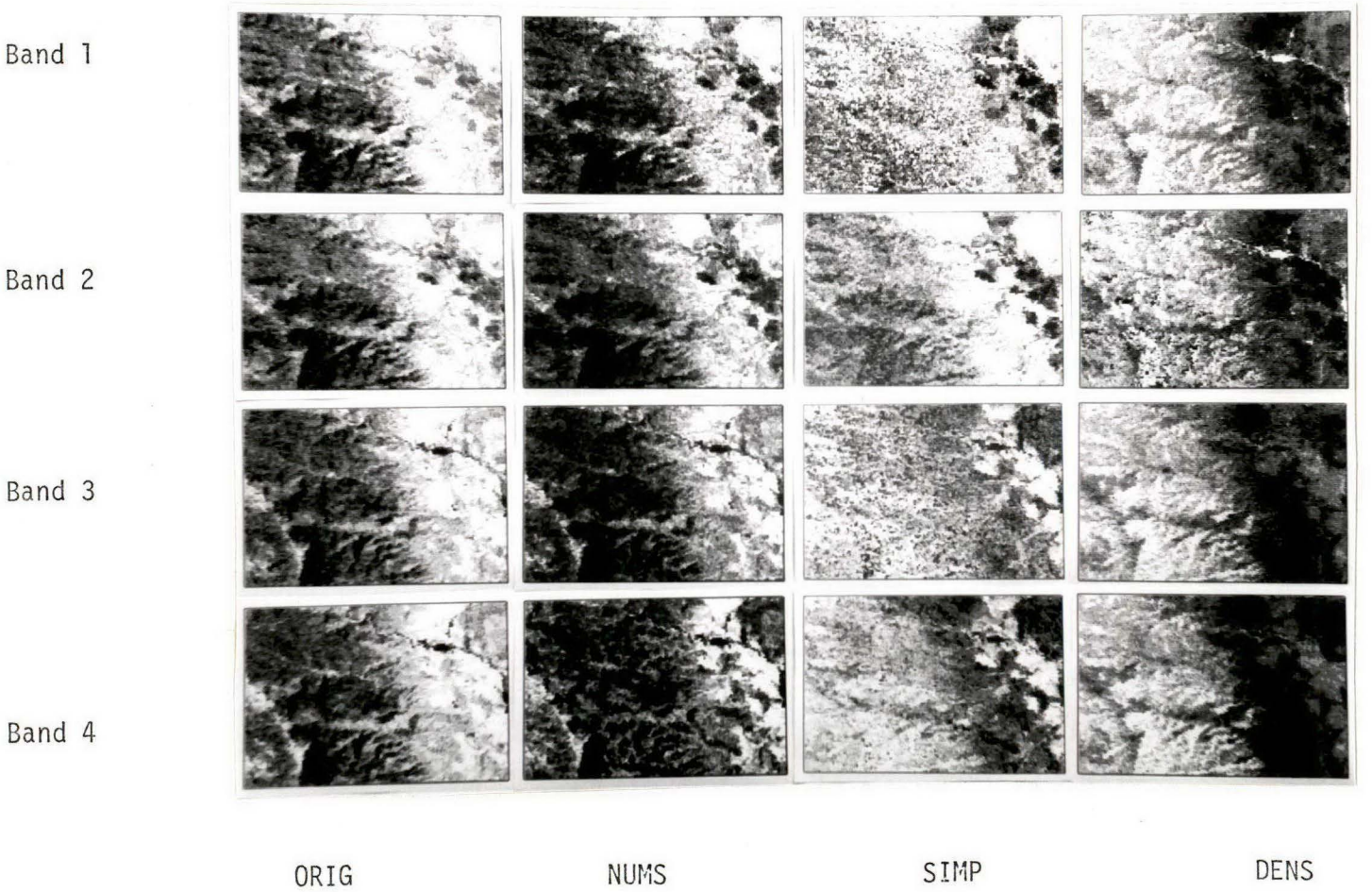

Figure 9. Grayscale displays of original and transformed data base files.

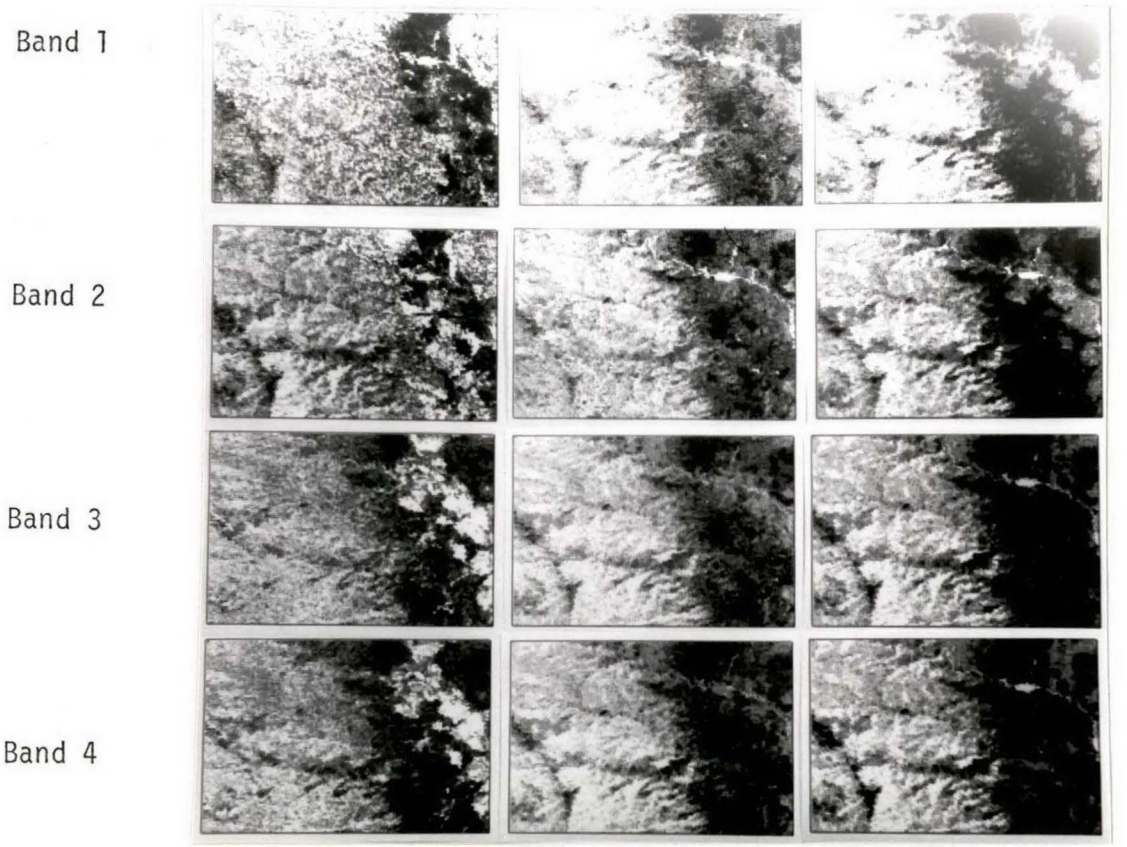

Figure 10. Grayscale displays of the difference data base files.

patterns across all bands in ΔS. This file, along with ΔD demonstrates that the information removed from Simp and Dens by transformation is overwhelming of similar nature in all bands, i.e. a brightness component. Nums, on the other hand, has a difference file, ΔN, which is highly variable between bands, showing that the Nums transformation has changed the spectral character of the original data.

It is interesting to note that of all the bands in these displays, band 2 of Simp is by far the best for viewing lineaments, especially the NNE/SSW trace running through the site in the western half. This feature traverses some of the heaviest topographic "grain" of the site, and while there are many shorter valley accordances evident on the aerial photos, this longer feature is quite obscured by topographic interference patterns on the photos.

Radiometric striping noise, caused by the imperfections in calibration for the six four-sensor arrays of Landsat, is most evident in band 1 of the original data. While in some cases it is difficult to see on the reduced displays provided, the striping pattern shows up in band 3 of the Simp file, band 4 of the Nums file, and bands 3 and 4 of the ΔN file. Elsewhere, the striping noise is not apparent. This is an example of a gradient effect; given the assumption that the noise is more spectrally dependent than brightness dependent, the Nums file, its difference resultant, and the Simp file can all be considered sensitive to subtle spectral variations. On the other hand, the Dens transformation, ΔS, and ΔN are accentuations of the brightness scene component, and mask the striping with a strong response to the average of all bands.

The random salt and pepper (high frequency/high amplitude) noise patterns are evident in all but band 2 of Simp, and only in band 2 of Dens. This "noise" could be a result of the color enhancement effects of transformation, with local ground reflectance variations being highly emphasized by the removal of a smoothing brightness element. The anomalous response of band 2 in the Simp and Dens files is possibly due to the lack of correlation between the original band 2 and the average brightness. This, in turn, may be caused by chlorophyll absorption in this scene containing locally vigorous vegetation near the peak of the growing season (July 10).

Many of the above indications are corroborated by the interband correlation analysis. Table 6 gives the correlation coefficients of each band pair, as well as a mean of coefficient absolute values, for each of the seven base files.

It is quite apparent from these data that there is a pervasive high correlation between bands in the original data. This has been noted by many investigators using Landsat data. While there are many factors which may play a part in this tendency towards correlation, it is certain that over this scene, with its highly variable illumination conditions, the topographic influence is one important contributor to the correlation.

The Simp transformation caused a negation of the correlations between visible and infrared bands, as expected upon color enhancement of a vegetated scene. There was also a decrease in correlation between the two visible-spectrum bands, and between the two infrared bands. These band pairs are those whose response would be most similar for a

Table 6. Interband correlation from site-wide sample: every 9th line and column.

Channel Pair:	1 vs. 2	1 vs. 3	1 vs. 4	2 vs. 3	2 vs. 4	3 vs. 4	Mean |r|
Original	.95	.75	.58	.72	.49	.88	.73
SIMP	.37	-.75	-.32	-.68	-.76	.49	.56
NUMS	.89	.33	.04	.38	-.01	.78	.41
DENS	.65	.71	.68	.47	.30	.85	.61
ΔS	.87	.93	.87	.83	.67	.91	.85
ΔN	.49	-.43	-.24	-.10	-.36	.47	.35
ΔD	.96	.95	.87	.90	.82	.95	.91

given irradiance; the drop in these correlations is additional evidence for the reduction of illumination dependence for the Simp file.

The Nums transformation failed to reduce illumination dependency in this respect. The 1 vs. 2 and the 3 vs. 4 coefficients were not significantly reduced. All other correlations were strongly suppressed, suggesting that color enhancement within the maintained illumination variation was achieved.

The Dens transformation showed reductions in correlation only for coefficients associated with band 2. This can be interpreted as an affirmation that band 2, of all the original bands, was the least correlated with the average. Logically, it seems that band 1 should be least correlated with the average, since it is affected least by topographic shadow. However, band 2 values are also affected more by skylight than are the infrared bands (see Figure 3), and so are less affected by topographic shadow. At the same time, band 2 shows strong irradiance absorption by chlorophyll, causing a definite inverse relationship to amount of productive vegetation. The combined effects of these two properties of band 2 make it a likely candidate for having the lowest correlation to the average. This could have been positively determined if the average values had been saved as an "extra" band.

Difference files for Simp and Dens showed correlation results which confirmed the optical impressions that the information change from these two transformations was overwhelmingly of shared brightness characteristics between the bands. However, the lowest coefficient in each case was for band 2 vs. 4, which could indicate a slight weakening effect by the averaging strategy on such inverse relationships

as chlorophyll red-band absorption with infrared reflectivity. This possibility needs quantitative evaluation.

ΔN had low coefficients throughout, which implies that the changes in data affected by Nums were, for practical purposes, independent of overall brightness. The similarity between correlations from Simp and ΔN indicates that much the same type of information was deleted by Nums as was retained by Simp, and suggests that the Nums transformation removed important information.

In summary, then, the optical and correlation outputs provided evidence from which the following conclusions can be made:

1. The Simp transformation has effectively reduced the brightness scene component, and has strengthened multivariate patterns associated with the spectral responses of vegetative cover.
2. The Nums and Dens transformations both failed to correct for topographic illumination variation. The Nums file shows a color enhancement potential while leaving the brightness patterns relatively unchanged, while the Dens file has changed the brightness component in an enhancement effect rather than in a normalization effect.

7.2 Training Data Analyses

The training data were samples from those categories delineated in Table 3. This classification was further stratified on the basis of illumination. Table 7 shows the codes for both vegetation and illumination strata and Table 8 gives symbol labels to each of the 36 classes defined within the training data.

Table 7. Coding system for training categories.

I. Vegetation (1st letter)

P closed conifer
A open crown conifer with lush understory
B very open crown conifer with lush understory
C open crown conifer with dry vegetative understory
D very open crown conifer with dry vegetative understory
R open crown conifer with rock understory
K very open crown conifer with rock understory
X excavated/disturbed/barren
G grassland/agriculture
T cottonwood/aspen
S mountain shrub
W water

II. Illumination (2nd letter)

B steep sloped and backlit
- gentle sloped and backlit
F steep sloped and frontlit
+ gentle sloped and frontlit
S steep sloped and sidelit
/ gentle sloped and sidelit

III. Vegetation Qualifiers

w/ C: + or - (3rd letter) denotes crown closure high/low within class range
w/ G: +/- (2nd letter) denotes high/medium/low producitivites
w/ S: +- (3rd letter) denotes high/low productivities

Table 8. Codes for the 36 training categories*

PS	- P:	steep, sidelit
P/	- P:	gentle, sidelit
PB	- P:	steep, backlit
P-	- P:	gentle, backlit
AS	- A:	steep, sidelit
A/	- A:	gentle, sidelit
AB	- A:	steep, backlit
AF	- A:	steep, frontlit
BS	- B:	steep, sidelit
B/	- B:	gentle, sidelit
BF	- B:	steep, frontlit
B+	- B:	gentle, frontlit
CS+	- C:	steep, sidelit, high crown closure
CS-	- C:	steep, sidelit, low crown closure
C/+	- C:	gentle, sidelit, high crown closure
C/-	- C:	gentle, sidelit, low crown closure
CF+	- C:	steep, frontlit, high crown closure
CF-	- C:	steep, frontlit, low crown closure
C++	- C:	gentle, frontlit, high crown closure
C+-	- C:	gentle, frontlit, low crown closure
DS	- D:	steep, sidelit
DF	- D:	steep, frontlit
RS	- R:	steep, sidelit
RB	- R:	steep, backlit
RF	- R:	steep, frontlit
KF	- K:	steep, frontlit
KS	- K:	steep, sidelit
X		no strata
G-	- G:	low productivity
G/	- G:	medium productivity
G+	- G:	high productivity
T		no strata
SS+	- S:	steep, sidelit, high productivity
SS-	- S:	steep, sidelit, low productivity
SF-	- S:	steep, frontlit, low productivity
W		no strata

* for vegetation codes and symbol system, see Table 7.

The categorical scheme as a whole was designed as a difficult testing ground for Landsat classification tests, such that the imperfection of the various files' responses would provide media for comparison of the transformations. However, the categorical scheme turned out to be detailed to an extent prohibitive of stable experimental conditions, as the accuracy figures discussed below will indicate. Nevertheless, from a purely comparative standpoint, the classification results show patterns of success and failure which are reasonable within this low accuracy context, and will therefore be addressed in full.

There were two sets of classification tests: one with the full 36-class structure, and another with the illumination strata of the 36-class group collapsed, resulting in a 16-class group. The difference between the two model sets was one of sample groupings; the same set of cells participated in each test. The 36-class test provided a controlling stratification that favored the un-normalized files in terms of class separability. The 16-class test was implemented to reverse the advantage, so that normalized data could be expected to perform with higher accuracies. However, since the models in the 16-class test were merely multimodal amalgamations of the original 36 samples, the test appears to favor each group in different ways; the un-normalized files are helped by an inclusion of all types of illumination conditions, while the normalized files have an advantage of overcoming much of the multimodality of the class models. In that the normalized files are not hindered by the inclusion of the illumination variation, they can be considered at a slight advantage in the 16-class test.

In terms of overall accuracies, the original data achieved the highest levels in both the 36 and 16-class tests. The Simp file was the worst performer in both cases. However, the proportion of Simp accuracy to original data accuracy improved in the 16-class test, whereas this did not happen for either the Nums or Dens cases (see below). The Simp accuracy was 44% less than original accuracy with 36 classes, but only 27% less with 16 classes. This change in relative accuracy suggests that some improvement was achieved by virtue of the change in illumination control. The remaining relative accuracy deficiency can be at least partially ascribed to the loss of the brightness component of reflectance.

No. of Classes	36				16			
	ORIG	NUMS	SIMP	DENS	ORIG	NUMS	SIMP	DENS
Overall Percent Accuracy	26.2	24.6	14.6	23.7	42.6	39.8	31.3	36.1
Portion of Highest Accuracy	1.00	.94	.56	.90	1.00	.93	.73	.85

In the mean brightness results (Table 9), there is strong corroborating evidence for the conclusions drawn from the site-wide analyses. The Nums file is very well correlated with the original file, whereas Simp has normalized these "mean means" to near midrange of the dynamic range, with a coefficient of variation of only 2.61%; this is a strong demonstration of the Simp algorithm's suppression of brightness variation. Dens, on the other hand, has evidently inverted the brightness patterns of the scene, with low radiance classes becoming high, and vice-versa.

Table 9. Training model mean brightness $B = (\sum_{i=1}^{4} \bar{X}_i)/4$

	ORIG	NUMS	SIMP	DENS
OVERALL	71	63	94	25
PS	32	32	92	43
P/	35	37	92	37
PB	19	20	92	76
P-	26	26	92	53
AS	34	31	93	43
A/	40	36	93	35
AB	35	30	94	42
AF	50	44	94	27
BS	59	51	94	24
B/	56	49	94	26
BF	73	63	94	19
B+	61	53	94	23
CS+	44	38	94	31
CS-	47	40	95	31
C/+	39	34	94	36
C/-	48	41	95	31
CF+	57	49	94	24
CF-	65	55	94	21
C++	51	44	94	27
C+-	57	49	94	25
DS	59	50	95	29
DF	75	63	95	20
RS	57	49	95	25
RB	26	24	93	65
RF	61	52	95	23
KF	88	76	95	17
KS	58	50	95	27
X	129	111	96	10
G-	121	103	96	11
G/	96	85	94	14
G+	102	102	92	12
T	95	92	93	14
SS+	90	77	95	16
SS-	90	76	95	16
SF-	106	90	96	13
W	39	51	87	53
C_{var}	40.46%	39.35%	2.61%	61.45%

The band variable F-values show little change in internal pattern between the 36-class and 16-class tests. For the 36-class values (Table 10), it is interesting to note that with original data, each band has a similar discriminant potential to start off with, but in the accumulated stepwise context, the collective discrimination is on a simplified visible/infrared function. This pattern is matched by Nums, with a slight added contribution from band 1, which indicates the subtle color enhancement of this transformation. The Simp file shows no very low F-values, but lacks the strong visible band contributor in the accumulated pattern. It is possible that since the 2 vs. 4 correlation was turned strongly negative, the discriminant potential of band 2 has been subordinated by the congruent and stronger band 4 potential. Also of consequence is the relationship of these two bands to the normalizing average. With higher correlation with the average would come increased spectral response amplification. Therefore, since band 2 is suspected of having low correlation to the average, its contribution is suppressed in the Simp file. However, band 4 may have high correlation to the average because it is affected more by both changes in vegetation and changes in topographic shadow. Therefore, it is not surprising that band 4 has the highest accumulated F-value for this file.

The results from individual training models can be split into summaries of mean vector, standard deviation, and coefficient of variation indicators, plus selected classification results with associated between class F-values.

Table 10. Band variable F-values.

Individual

Band	ORIG	NUMS	SIMP	DENS
1	145	121	65	68
2	158	144	98	50
3	156	157	69	94
4	160	169	102	84

Accumulated Stepwise

Band	ORIG	NUMS	SIMP	DENS
1	9	23	17	55
2	161	144	23	13
3	5	8	22	94
4	160	169	102	7

The mean vectors for all files were plotted per class. These plots are contained in Figures 10 through 12. They reaffirmed that: 1) Simp normalizes the spectral curves to midrange, 2) Dens inverts overall brightness, and 3) Nums is quite similar to the original file, except that the plot shape has been amplified somewhat. The Simp file shows far greater curve amplitudes than any of the other files; this suggests that this file may have outperformed the others if subsequent simple ratio techniques had been employed. The Dens file has plotted out with a tendency towards flat curves, indicating that its discriminant potential is based on brightness differences between the classes; the exceptions to this are in the backlit categories whose spectral shapes were emphasized upon the inversion to bright levels.

Standard deviation changes from the original to Simp file (Table 11) were associated primarily with the original brightness of the given model, and secondarily with the presence of multispectral variation or color within the model.

The brightness dependency takes the pattern of increased s for originally low radiance classes, and decreased s for originally high radiance classes. While this can be attributed to the shift in mean controlling the magnitude of deviation, other causative factors undoubtedly play a part. In particular, the changing proportion of color and brightness contributions to the model mean can also explain the changes in standard deviation. With Simp's normalization of brightness to midrange, and its accentuation of multispectral response, one would expect color variation, which had been suppressed by low brightness, to express itself more strongly after transformation. The drop

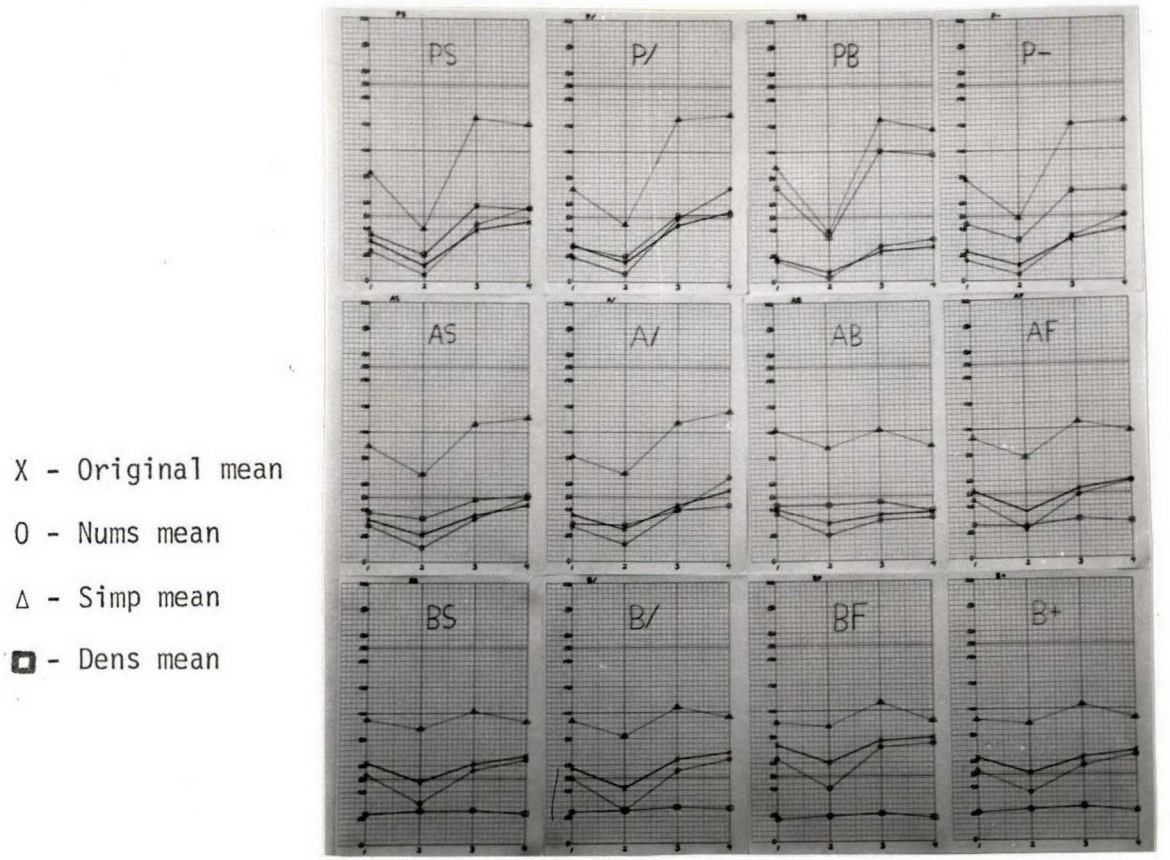

Figure 11. First set of 12 spectral plots of training model mean vectors for original and transformed files.

X - Original mean

O - Nums mean

Δ - Simp mean

□ - Dens mean

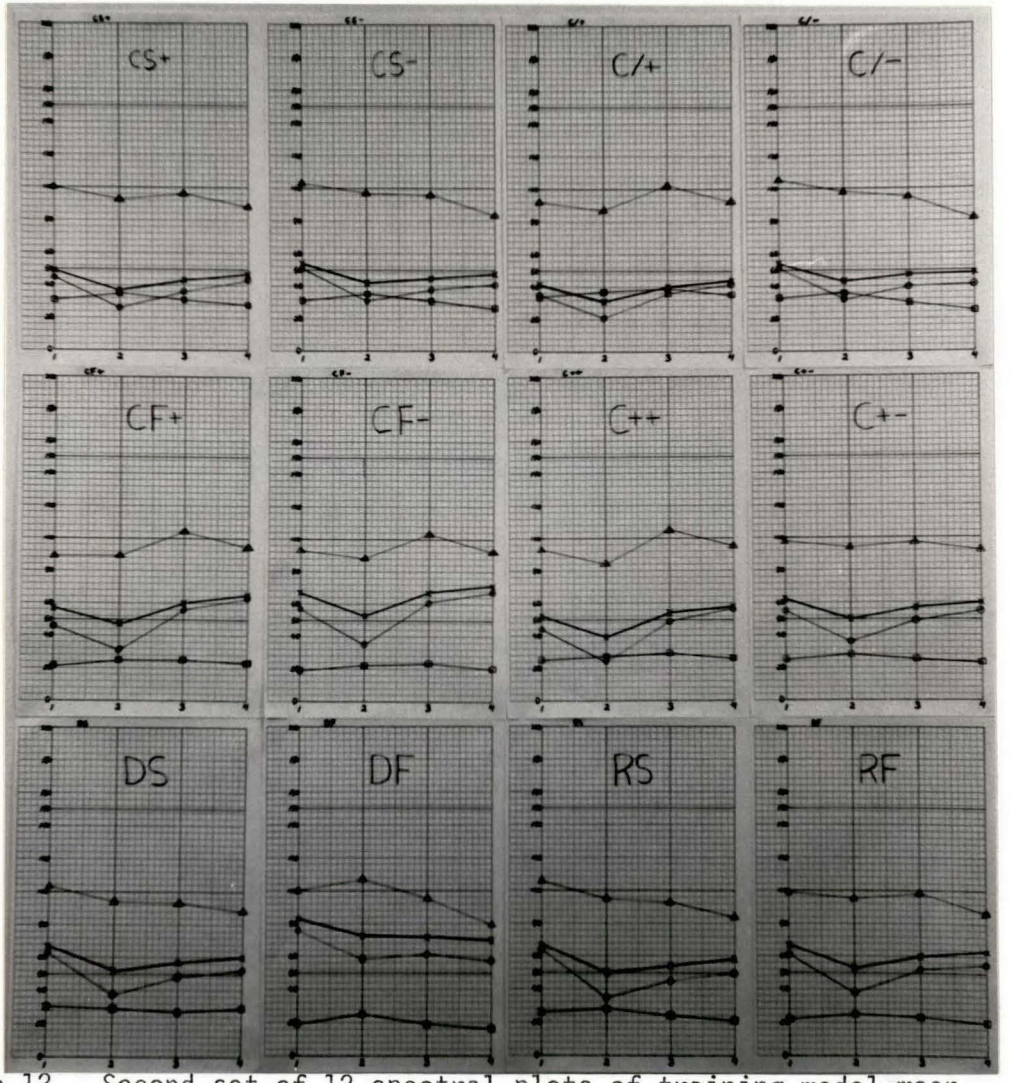

Figure 12. Second set of 12 spectral plots of training model mean vectors for original and transformed files.

X - Original mean

O - Nums mean

Δ - Simp mean

□ - Dens mean

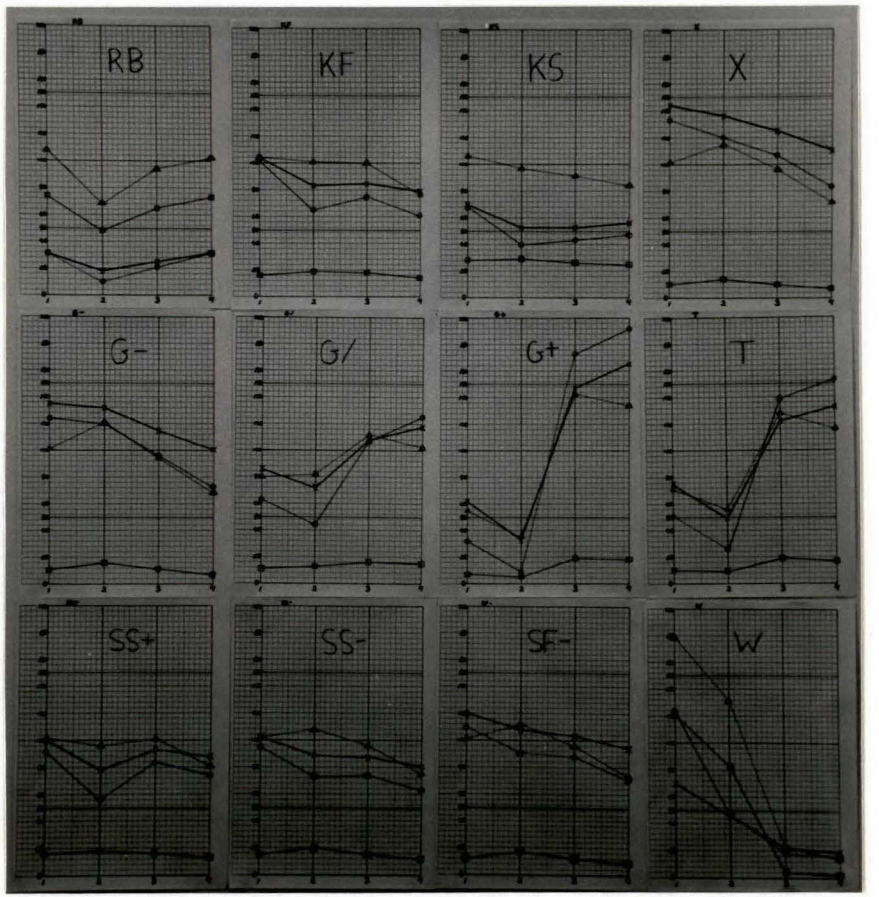

Figure 13. Third set of 12 spectral plots of training model mean vectors for original and transformed files.

Table 11. Change in standard deviation in training models from original to transformed files.

	NUMS				SIMP				DENS			
Band	1	2	3	4	1	2	3	4	1	2	3	4
PS	+3	-2	+6	+9	+12	+14	+12	+10	+3	0	+8	+10
P/	0	-3	+4	+10	+9	+11	+8	+13	-3	-4	+5	+8
PB	+3	-3	+6	+6	+26	+29	+30	+16	+31	+33	+36	+38
P-	+1	-2	+5	+9	+11	+19	+10	+10	+10	+10	+11	+10
AS	+2	-3	+1	+5	+6	+4	+2	+7	-1	-2	+6	+9
A/	+2	-2	+4	+6	+6	+6	+4	+5	-3	-2	-1	+2
AB	+1	-1	-1	+2	+1	+8	+4	+3	+4	+4	+9	+4
AF	+2	-2	+1	+1	-1	+3	-2	+2	-8	-8	-5	-2
BS	+1	-1	+3	+3	-4	-2	-8	-8	-8	-6	-13	-11
B/	0	-2	+2	+2	-4	-2	-8	-7	-5	-4	-10	-5
BF	+2	-1	-1	+1	-11	-6	-6	+3	-17	-18	-8	-3
B+	+2	-1	+1	+4	-4	+3	0	+4	-12	-13	-5	-3
CS+	+5	0	+1	+3	+3	+5	+2	+2	-4	0	-1	-4
CS-	+2	0	0	+2	-2	-1	0	+1	-7	-6	0	-3
C/+	+1	-2	+3	0	+4	+7	+7	+1	0	-2	+3	+3
C/-	0	-1	0	+1	-2	+1	-8	-5	-2	-6	-10	-10
CF+	+2	0	+4	+5	-2	+3	0	+1	-7	-4	-5	-4
CF-	+1	-1	+1	+1	-9	-4	-4	-3	-12	-10	-7	-5
C++	+2	-1	+5	+4	+4	+2	0	0	-3	-2	-8	-4
C+-	-1	-2	+1	0	-6	-9	-11	-6	-10	-14	-13	-9
DS	0	-3	-2	-3	-18	-5	-12	-1	-2	-7	-7	+14
DF	+2	-2	-2	-3	-18	-14	-13	-8	-19	-15	-16	-10
RS	+3	-1	+1	+1	-4	-3	-3	-2	-6	-7	-8	-5
RB	+3	-3	-1	+1	+10	+12	+3	+8	+31	+14	+24	+33
RF	+2	-1	0	0	-7	-4	-5	-2	-11	-10	-6	-4
KF	+5	-3	-1	+1	-15	-4	-1	+1	-26	-18	-4	-4
KS	+5	-3	-2	-2	-15	-5	-7	+4	-15	-13	-4	+8
X	+6	+9	+4	+10	-17	-16	-11	-5	+26	-33	-19	-18
G-	+3	+4	+1	+2	-11	-14	-20	-19	-20	-23	-25	-27
G/	+1	-1	+5	+8	-10	-6	-9	-12	-16	-14	-14	-17
G+	0	-6	0	-9	-2	0	-14	-14	-10	-11	-22	-21
T	+5	-3	+16	+16	-4	0	-7	-10	-20	-24	-22	-30
SS+	+1	0	+3	+1	-11	-8	-12	-11	-16	-15	-19	-18
SS-	+4	+2	+1	0	-13	-12	-9	-6	-19	-20	-15	-12
SF-	+3	+3	+1	+1	-9	-7	-8	-6	-14	-14	-12	-11
W	+3	0	-3	-3	+13	+3	-4	-9	+44	+6	-37	-38

in standard deviation for the bright/frontlit classes can be explained by a suppression effect upon brightness variation, which was of greater magnitude than color variation in the original data.

The brightness normalization of the transformation would tend to smooth variation in less colorful classes. This is the case for the C class grouping, wherein the categories with lower crown closure have much flatter curves than the higher crown closure categories. The standard deviations were generally reduced for the former cases, and increased for the latter.

The coefficients of variation calculations (Table 12) were undertaken to remove the uncertainty of the standard deviation response relative to the mean level. It is evident from Simp's drastic reduction of coefficients of variation on all categories, that this transformation has reduced brightness variation even within a given strata, and may have reduced other multiplicative noise sources as well.

Individual category classification performances are highly variable across the category list, and are difficult to interpret because of the complex interdependencies of one class's performance on the results obtained from associated classes. The usual interdependency of classification results caused by the intersection of probability surfaces is enhanced by the use of a shared covariance matrix in the testing algorithm. Furthermore, dependencies change from file to file, and this lack of control is compounded by the dissimilarities in original sample distributions. Unfortunately, the highly detailed nature of the categorical structure only perturbs these analyses further.

Table 12. Coefficients of variation ($s/\bar{x}$ in percent) for individual training models.

		ORIG	NUMS	SIMP	DENS			ORIG	NUMS	SIMP	DENS			ORIG	NUMS	SIMP	DENS
PS	1	35	54	26	35	CS+	1	24	35	15	22	RF	1	24	30	9	22
	2	82	158	61	55		2	21	31	14	23		2	27	37	12	19
	3	25	36	17	31		3	19	24	11	25		3	20	23	8	25
	4	23	33	18	38		4	22	33	14	21		4	17	20	10	33
P/	1	39	60	28	31	CS -1		31	37	14	31	KF	1	30	35	15	24
	2	72	133	50	37		2	38	52	16	31		2	31	37	22	42
	3	19	26	13	27		3	28	32	13	41		3	20	22	17	74
	4	15	25	16	30		4	31	39	19	44		4	20	27	22	79
PB	1	47	71	39	57	C/+	1	27	34	17	32	KS	1	40	49	12	48
	2	102	143	92	114		2	35	46	22	24		2	42	50	18	31
	3	43	61	33	47		3	27	38	17	34		3	34	37	13	58
	4	37	47	22	43		4	19	21	10	32		4	25	23	21	85
P-	1	34	54	23	40	C/-	1	30	31	13	42	X	1	19	26	10	20
	2	63	104	54	57		2	41	49	18	32		2	26	38	17	21
	3	34	44	17	31		3	42	49	12	32		3	17	23	11	22
	4	32	43	18	32		4	41	50	17	37		4	19	37	21	34
AS	1	38	54	20	29	CF+	1	17	24	8	14	G-	1	16	18	9	22
	2	48	70	22	24		2	22	34	14	18		2	20	26	11	21
	3	33	38	14	37		3	16	23	9	15		3	23	29	7	21
	4	26	31	16	41		4	13	22	10	19		4	29	42	14	27
A/	1	36	55	23	35	CF-	1	24	31	9	21	G/	1	22	30	11	23
	2	42	64	24	29		2	27	38	12	18		2	25	38	13	22
	3	27	38	14	26		3	19	22	8	25		3	17	22	9	25
	4	21	26	14	31		4	16	18	10	31		4	18	22	9	25
AB	1	34	41	15	42	C++	1	18	26	14	25	G+	1	21	38	20	29
	2	45	60	25	41		2	20	26	11	20		2	39	74	39	44
	3	31	34	15	46		3	25	35	13	18		3	17	15	8	14
	4	31	38	16	41		4	18	25	12	23		4	15	8	8	18
AF	1	28	36	14	27	C+-	1	28	29	12	28	T	1	32	58	28	43
	2	37	55	21	19		2	42	56	14	29		2	60	104	53	59
	3	23	29	10	26		3	35	42	9	27		3	21	31	15	23
	4	17	20	12	31		4	28	31	12	30		4	26	33	21	24
BS	1	25	31	12	33	DS	1	38	41	8	81	SS+	1	22	26	12	41
	2	29	39	13	29		2	43	50	19	50		2	27	38	14	37
	3	31	40	11	26		3	40	46	12	59		3	25	31	12	25
	4	29	32	11	31		4	32	30	20	117		4	24	29	14	31
B/	1	27	31	12	40	DF	1	32	36	9	40	SS-	1	22	27	10	24
	2	33	43	13	37		2	32	36	9	36		2	27	36	12	22
	3	32	37	11	29		3	30	34	9	32		3	21	26	10	24
	4	28	31	11	51		4	25	25	11	44		4	18	25	13	33
BF	1	27	37	10	17	RS	1	24	29	11	38	SF-	1	13	16	6	15
	2	31	41	15	10		2	28	37	12	26		2	15	22	9	15
	3	17	18	8	24		3	27	34	12	27		3	13	17	6	14
	4	11	15	13	37		4	23	29	13	39		4	13	18	8	16
B+	1	26	35	13	24	RB	1	53	59	25	65	W	1	41	27	23	60
	2	36	50	24	21		2	73	91	38	58		2	79	75	30	51
	3	20	24	12	32		3	53	57	18	57		3	195	227	166	148
	4	16	25	16	35		4	48	52	24	65		4	226	244	213	215

Nevertheless, there are patterns of performance shifts which do shed light upon the effects of the Simp transformation, and to that degree a discussion of selected cases is warranted.

First of all, the Simp transformation increased classification accuracy for those categories whose subtle spectral response was masked by a large brightness variation. Within this particular training categorical structure, then, these classes' separability was hindered by brightness information. For example, low productivity grassland (G-) had a self-classification accuracy which rose from 49% to 60% after Simp transformation. While the Type I confusion with steep, frontlit, low productivity mountain shrub (SF-) was reduced, the same type of confusion was increased, to a lesser degree, with steep frontlit, very open, dry vegetated understory conifer (DF). In terms of F- value, with the original data, G- had between-class F's below 100 for only the following classes: DF, very open conifer with rocky understory steep frontlit (KF), disturbed (X), and the mountain shrubs (S's); all these values were around 60, except for SF-, which was 20, and X, which was 6. For the Simp file, though, 75% of the F-values were <u>below</u> 50, with five well below 10. This shows that the Simp transformation, while improving classification in a few cases, has removed information which is useful for category discrimination within such a detailed categorical scheme. This impression can be extended to the A, B, C, D gradient of conifer stands as well.

The closed crown conifer group (P) as a whole has strong spectral response which was confounded heavily by topographic shadow. The original data showed confusion between these P strata and most other conifer strata. On the Simp data test, however, most of the

between conifer class F-values were increased, in spite of the fact that general F-value levels for Simp were far lower. A slight confusion with high productivity grassland and cottonwood/aspen was introduced in the 36-class test, and became a serious error source in the 16-class test. It is significant that brightness normalization removed confusion with closely associated classes, but introduced problems with unrelated classes which originally had been discriminated on the basis of brightness.

Open conifer with rocky understory steep backlit (RB) constitutes one of the few predictable performers of the category set. In the original data it performed at 13% accuracy, confused with closed conifer steep backlit (PB) by 32% Type I error, with open conifer lush understory steep backlit (AB) by 13% Type I error, and with P-, AS, KS, and C/+ classes[2] by 6% Type I errors. After Simp transformation, its accuracy rose to 33%, with Type I errors with much the same categories, but to a far lesser extent: P- by 13%, PB by 10%, DS by 10%, and AS by 6%. The error introduction associated with very open conifer dry vegetated understory steep sidelit (DS) is somewhat surprising considering the spectral differences between the two stand compositions. The spectral bias associated with the brightness

---

[2] P- is closed conifer gentle backlit, AS is open conifer lush understory steep sidelit, KS is a very open conifer rock understory steep sidelit, and C/+ is open conifer dry vegetated understory gentle sidelit.

normalization could well have impaired the spectral differentiation of these two classes. However, overall it can be said that the removal of topographic shadow effects has enhanced the detailed character of the spectral response for RB.

A comparison of the KS and KF categories'[3] classification results provides an overall impression of the utility of the tests. KF had 39% and 33% accuracies for original and Simp files, while KS had 19% and 6% respectively. The K class in the 16-class test, however, showed higher accuracy for the Simp file, but only by 24% to 15% for the original. Patterns of confusion did not shift appreciably from original to transformed in either test. However, even though the accuracy relationship for the files reversed between the two tests, F-values for the two classes were consistently lower in the Simp portion of both tests. This pattern of reduced F-values in spite of the occasional gain in accuracy for the Simp file can be explained by the following logic: while the transformation reduced the variance within the class, the collection of the class clusters was compressed in feature space by the elimination of brightness information. This between class compression seems to have overridden the advantages of spectral enhancement and variance reduction, resulting in lower F-values and poorer overall classification results for the Simp file.

Finally, the classification results should be interpreted with the understanding that both the categorical stratification and the shared covariance matrices tended to bias the comparative analyses.

---

3 K stands for very open rocky understory conifer, S denotes steeply sidelit and F is steeply frontlit.

If the tests were structured with singular unstratified cover type models and with an individual covariance matrix algorithm, the results for the Simp transformation would likely change in comprison with those from the original data.

7.3 Collation of Results

The following significant results can be generalized from this study:

1. There was relatively little effect on brightness patterns by the Nums transformation, a strong brightness normalization by the Simp transformation, and an inversion of brightness patterns by the Dens transformation.
2. Along with the brightness normalization was an enhancement of spectral response by the Simp transformation. There were indications that this enhancement was most effective for highly correlated original bands, and least effective for inverse relationships such as the red/IR response of vegetation.
3. Classification tests showed that:
   a. F values between classes in the tests dropped in almost all cases after brightness normalization.
   b. After Simp transformation, accuracies rose for some between-class distinctions which were based upon subtle spectral difference detection, and accuracies fell for class distinctions based on brightness magnitude.
   c. Accuracies were, as a rule, degraded by the loss of brightness information.

8.0 SUMMARY AND CONCLUSIONS

While this research was only a portion of a more comprehensive experimental design, there are many results which give strong evidence to the nature of the effects of the Simp transformation on classification of cover types in rugged terrain. The objectives as stated in Section 5.1 were achieved, namely that the beneficial and negative effects were evaluated, and that the degree of illumination normalization was assessed.

The first hypothesis, that vegetation cover types are separable solely on the basis of color or spectral character, was not supported by the results obtained. The comparison of classification results showed that, for this particular categorical scheme, brightness was a more valuable scene component than was color for classification of vegetation cover types. While this held true for these tests, results could change with different class schemes and different classification algorithms.

Hypothesis number two, that the Simp transformation would eliminate brightness variation and enhance spectral response, was confirmed consistently throughout the results. In addition to the indicators associated with Simp, the gradient of under and over-correction of brightness in the Nums and Dens files supported the impressions of the primary effect, and eliminated suspicions of coincidental results.

The third hypothesis predicted classification improvement for classes separated by subtle spectral differences, and classification degradation between classes discriminated by brightness differences.

First, the improvement of spectral detectability is subject to question. While some supporting cases were documented, the trade-off between reduced between-class F-values and reduced within-class variance, in the test cases studied, seemed unfavorable to improved accuracy; the between-class F's were reduced too far to take advantage of the enhancement of the spectral characteristics of each class model. The shared covariance algorithm of the classifier failed to take full advantage of the spectral enhancement, and, therefore, the extent of potential classification improvement due to such enhancement is as yet unassessed.

Nevertheless, the dominant conclusion from these results derives from the stable pattern of a drop in discrimination potential after brightness normalization. The between-class F-values were invariably lower, and the trend in reduction of accuracy extended beyond brightness separabilities and into the spectrally distinguished classes. Overall, the cost in terms of information loss outweighed any advantages of brightness normalization or spectral enhancement effects.

In conclusion, the transformation holds few advantages for digital processing in the context of the categories and algorithms used in this research. However, there may be other circumstances under which brightness normalization is a useful preprocessing tool. In particular, for geological applications where topographic or soil/rock brightness variation may be masking more significant spectral differences, the Simp transformation could be useful. Even in the case of cover type inventory, a suppression of brightness variation may be helpful if the underlying spectral patterns were sufficiently distinct. Finally, in terms of more general remote sensing applications, a potential

has been affirmed by this study for separating the brightness and spectral scene components, resulting in a data configuration which might be used more effectively to extract information related uniquely to each of the components.

REFERENCES CITED

Ali, M., and J.K. Aggarwhal, 1976. Automatic detection and classification of infestations of crop insect pests and diseases from infrared color aerial photographs. Proc. of LARS Symp. on Machine Processing of Remotely Sensed Data, 1976, pp. 4B1-4B11.

Billingsley, F.C., and A.F.H. Goetz, 1973. Computer techniques used for some enhancements of ERTS images. Proc. of Symp. on Significant Results from ERTS-1, Goddard Space Flight Center, Greenbelt, Md., March, 1973, Vol. I, Sec. B, pp. 1159-1167.

Billingsley, F.C., 1973. Some digital techniques for enhancing ERTS imagery. Proc. of Symp. on Management and Utilization of Remotely Sensed Data, American Society of Photogrammetry, Sioux Falls, S.D., Oct., 1973, pp. 284-293.

Brooner, W.G., and D.S. Simonett, 1971. Crop discrimination with color infrared photography, a study in Douglas County, Kansas. Remote Sensing of Environment, Vol. 2, pp. 21-35.

Chavez, P.S., Jr., and W.B. Mitchell, 1976. Computer enhancement techniques of Landsat MSS digital images for land use/land cover assessments. USGS Internal Note (personal copy obtained from Dr. Chavez).

Colwell, J.E., 1974. Vegetation canopy reflectance. Remote Sensing of Environment, Vol. 3, pp. 175-183.

Crane, R.B., 1971. Preprocessing techniques to reduce atmospheric and sensor variability in multispectral scanner data. Proc. of the 7th Int. Symp. on Remote Sensing of Environment, V. II, pp. 1345-1355.

Duggin, M.J., 1974. On the natural limitation of target differentiation by means of spectral discrimination techniques. Proc. of the 9th Int. Symp. on Remote Sensing of Environment, V. I, pp. 499-513.

Gillespie, Allen, 1977. Personal communication. Jet Propulsion Laboratory, Pasadena, California.

Hansen, J.H., 1975. The effects of preprocessing transformations on image discrimination. Remote Sensing of Earth Resources, F., V.IV, F., Shahrokhi, ed., Univ. of Tenn. Space Institute, Tullahoma, Tenn., pp. 1-19.

Hulstrom, R.L., 1973. The cloud bright spot. Photogrammetric Engineering, Vol. 39, No. 4, April, 1973, pp. 370-376.

Kreigler, F.J., W.A. Malila, R.F. Nalepka, and W. Richardson, 1970. Preprocessing transformations and their effects on multispectral recognition. Proc. of the 6th Int. Symp. on Remote Sensing of Environment, V. I, pp. 97-131.

Maxwell, E.L., A. Morse, and N. Schmidt, 1978. User's manual for LANDSAT digital data classification of land use and wildlife habitat inventory. Bendix Aerospace Systems Division/Colorado State University Final Report for Fish and Wildlife Service, Office of Biological Services Contract 14-16-0008-2160, 55p., (in press).

Nalepka, R.F., 1970. Investigation of multispectral discrimination techniques. Institute of Science and Technology, Univ. of Mich. Press, Ann Arbor, Mich., pp. 13-27.

Podwysocki, M.H., E.J. Gunther, and H.W. Blodget, 1977. Discrimination of rock and soil types by digital analysis of Landsat data. NASA Goddard Space Flight Center, Greenbelt, Md., Preprint X-923-77-17, Jan., 1977, 37p.

Ross, D.S., 1973. Atmospheric effects on multispectral photographs. Photogrametric Engineering, Vol. 39, No. 4, April, 1973, pp. 377-384.

Rouse, J.W., Jr., R.H. Haas, J.A. Schell, D.W. Deering, and J.S. Harlan, 1974. Monitoring the vernal advancement and retrogradation (greenwave effect) of natural vegetation. NASA Goddard Space Flight Center Type III Final Report, NASA Contract 5-21857, Nov., 1974, 371p.

Rowan, L.C., P.H. Wetlaufer, and A.F.J. Goetz, 1976. Discrimination of rock types and detection of hydrothermally altered areas in south central Nevada. In ERTS-1, A New Window on Our Planet, USGS Professional Paper 929, R.S. Williams and W.D. Carter, eds., pp. 102-105.

Siegal, B.S., and M.J. Abrams, 1976. Geological mapping using Landsat data. Photogrammetric Engineering and Remote Sensing, Vol. 42, No. 3, March, 1976, pp. 325-337.

Smedes, H.W., 1971. Automatic computer mapping of terrain. Proc. of the Int. Workshop on Earth Resources Survey Systems, V. III, pp. 345-406.

Smedes, H.W., M.M. Spencer, and F.J. Thomson, 1971. Preprocessing of multispectral data and simulation of ERTS data channels to make computer terrain maps of a Yellowstone National Park test site. Proc. of the 7th Int. Symp. on Remote Sensing of Environment, V. III, pp. 2073-2090.

Thrower, N.J.W., and R.V. Cooke, 1968. Scales for determining slopes from topographic maps. The Professional Geographer, Vol. XX, No. 3, May, 1968, pp. 181-186.

Tucker, C.J., 1977. Use of near infrared/red radiance ratios for estimating vegetation biomass and physiological status. NASA Goddard Space Flight Center, Greenbelt, Md., Prepring #X-923-77-183, July, 1977, 41p.

Vincent, R.K., 1972. An ERTS multispectral scanner experiment for mapping iron compounds. Proc. of the 8th Int. Symp. on Remote Sensing of Environment, V. II, pp. 1239-1247.

Vincent, R.K., 1973. Spectral ratio imaging methods for geological remote sensing from aircraft and satellites. Proc. of Symp. on Management and Utilization of Remotely Sensed Data, American Society of Photogrammetry, Sioux Falls, S.D., Oct., 1973, pp. 377-397.

Wagner, T.W., R. Dillman, and F. Thompson, 1973. Remote identification of soil conditions with ratioed multispectral data. Remote Sensing of Earth Resources, V. II, F. Shahrokhi, ed., Univ. of Tenn. Space Institute, Tullahoma, Tenn., pp. 721-737.

Williams, D.H., and J.K. Aggarwhal, 1976. Computer location of citrus trees using color aerial infrared transparencies. Proc. of LARS Symp. on Machine Processing of Remotely Sensed Data, 1976, pg. 3B-2.

Yost, E., and S. Wenderoth, 1969. Ecological applications of multispectral color aerial photography. In Remote Sensing in Ecology. Phillip Johnson, ed., University of Georgia Press, Athens, Ga., 1969, pp. 46-62.

Yost, E., R. Anderson, and A.F.H. Goetz, 1973. Isoluminous additive color method for the detection of small spectral reflectivity differences. Photographic Science and Engineering, Vol. 17, No. 2, March/April, 1973, pp. 177-182.